

AD-752 061

GENERATION OF ARTIFICIAL GEOMAGNETIC
MICROPULSATIONS WITH A LARGE GROUND-
BASED CURRENT LOOP

A. C. Fraser-Smith, et al

Stanford University

Prepared for:

Office of Naval Research
Advanced Research Projects Agency

June 1972

DISTRIBUTED BY:

NTIS

National Technical Information Service
U. S. DEPARTMENT OF COMMERCE
5285 Port Royal Road, Springfield Va. 22151

Generation of Artificial Geomagnetic Micropulsations with a Large Ground-Based Current Loop

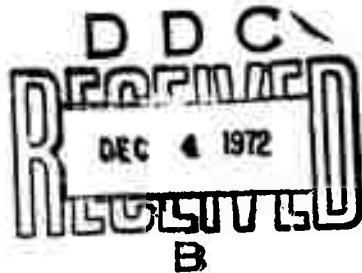
by

A. C. Fraser-Smith
Kenneth J. Harker
Robert T. Bly, Jr.
David M. Bubenik

June 1972

Approved for public release; distribution unlimited.

Technical Report No. 4



Sponsored by

Defense Advanced Research Projects Agency
(ARPA Order No. 1733; Program Code No. 2E20)
through the Office of Naval Research
Contract No. N00014-67-A-0112-0066

Reproduced by
**NATIONAL TECHNICAL
INFORMATION SERVICE**
U S Department of Commerce
Springfield VA 22151

RADIOSCIENCE LABORATORY

STANFORD ELECTRONICS LABORATORIES

STANFORD UNIVERSITY • STANFORD, CALIFORNIA



AD 752061

95

Principal Investigator:

O. G. Villard, Jr.
(415) 321-2300

Scientific Officer:

Director, Field Projects Programs
Code 418
Office of Naval Research
Arlington, Virginia 22217

The views and conclusions contained in this document are those of the author and should not be interpreted as necessarily representing the official policies, either expressed or implied, of the Defense Advanced Research Projects Agency or the U. S. Government

ACCESSION for		
NTIS	White Section	<input checked="" type="checkbox"/>
DDC	Buff Section	<input type="checkbox"/>
UNANNOUNCED		<input type="checkbox"/>
JUSTIFICATION.....		
BY.....		
DISTRIBUTION/AVAILABILITY CODES		
Dist.	AVAIL.	and/or SPECIAL
A		

DOCUMENT CONTROL DATA - R & D

(Security classification of title, body of abstract and indexing annotation must be entered when the overall report is classified)

1. ORIGINATING ACTIVITY (Corporate author) Stanford Electronics Laboratories Stanford University Stanford, California 94305		2a. REPORT SECURITY CLASSIFICATION UNCLASSIFIED	
		2b. GROUP -----	
3. REPORT TITLE GENERATION OF ARTIFICIAL GEOMAGNETIC MICROPULSATIONS WITH A LARGE GROUND-BASED CURRENT LOOP			
4. DESCRIPTIVE NOTES (Type of report and inclusive dates) Technical Report covering the period January 1971 through June 1972			
5. AUTHOR(S) (First name, middle initial, last name) A. C. Fraser-Smith, Kenneth J. Harker, Robert T. Bly, Jr., and David M. Bubenik			
6. REPORT DATE June 1972		7a. TOTAL NO. OF PAGES 118	7b. NO. OF REFS 44
8a. CONTRACT OR GRANT NO. Contract N00014-67-A-0112-0066		9a. ORIGINATOR'S REPORT NUMBER(S) Technical Report No. 4 SU-SEL-72-023	
b. PROJECT NO. ARPA Order No. 1733; Program Code 2E20		9b. OTHER REPORT NO(S) (Any other numbers that may be assigned this report) ----	
10. DISTRIBUTION STATEMENT Approved for public release; distribution unlimited.			
11. SUPPLEMENTARY NOTES Sponsored by ARPA and monitored by ONR (Code 418)		12. SPONSORING MILITARY ACTIVITY Office of Naval Research Field Projects Programs, Code 418 Arlington, Virginia 22217	
13. ABSTRACT The purpose of this study is to investigate and, if possible, establish the feasibility of producing artificial geomagnetic micropulsations by using a large horizontal current loop on the ground. Most natural micropulsations appear to be produced by hydromagnetic (hm) waves propagating in the ionosphere and/or the magnetosphere, and the term "artificial micropulsations" is used to mean artificially produced hm waves with propagation characteristics similar to those of the natural signals. The critical quantity in the generation process for the hm waves is the amplitude of the magnetic field variation that can be produced in the ionospheric E-region by the ground-based loop. Currents are induced in the conducting earth beneath the loop whenever its current is varied, and these currents have a magnetic field opposing the magnetic field of the loop. If either the conductivity of the earth or the variation frequency is too high the field at E-region heights may be reduced to a level where negligible hm wave amplitudes are produced. The effect of these earth currents is calculated for an assumed single-layer earth and for a wide range of frequencies (10^{-2} - 10^2 Hz) and earth conductivities (10^{-5} - 4 mho/m). It is found that at 1 Hz and for a conductivity of 10^{-4} mho/m (representing a typical conductivity for the earth's crust) the magnetic field of the loop is reduced by about 18 percent. At lower frequencies the reduction in magnetic field is even less. Thus, provided the loop is suitably located, the effect of earth currents should not be very great. (continued on page 2)			

14. KEY WORDS	LINK A		LINK B		LINK C	
	ROLE	WT	ROLE	WT	ROLE	WT
<p>micropulsations artificial micropulsations current loop earth currents hydromagnetic waves ionosphere magnetosphere</p> <p><u>ABSTRACT (Cont)</u></p> <p>Expressions for the two hm wave modes excited in the ionosphere by a current loop on the ground are derived and the feasibility of constructing large current loops is considered. It is concluded that current loops with magnetic moments as large as 7×10^{13} amp.m² are practicable and that the current in these loops can be varied at micropulsation frequencies. All things considered, the total magnetic field produced in the D-region could have an amplitude as large as 0.5 gamma, which is greater than most natural micropulsation amplitudes observed beneath the ionosphere.</p> <p>Preliminary calculations with the expressions for the two hm wave modes indicate that significant hm wave amplitudes can be produced in the ionosphere above the larger current loops considered in this study. This conclusion is independently confirmed by Greifinger (1972). Thus, we conclude that the artificial generation of micropulsations is feasible and that a large current loop should be capable of producing observable Pc 1 micropulsations at very considerable distances (greater than 5000 km) from the source. Much further study is required to establish all the possibilities of the artificial generation process, particularly at low micropulsation frequencies and for field-line propagation. However, a number of important uses for artificially-generated micropulsations are immediately apparent and are discussed briefly.</p> <p style="text-align: center;">Ib</p>						

**GENERATION OF ARTIFICIAL GEOMAGNETIC MICROPULSATIONS
WITH A LARGE GROUND-BASED CURRENT LOOP**

by

**A. C. Fraser-Smith
Kenneth J. Harker
Robert T. Bly, Jr.
David M. Bubenik**

June 1972

Technical Report No. 4

Sponsored by

**Defense Advanced Research Projects Agency
(ARPA Order No. 1733; Program Code No. 2E20)
through the Office of Naval Research
Contract No. N00014-67-A-0112-0066**

II

ABSTRACT

The purpose of this study is to investigate and, if possible, establish the feasibility of producing artificial geomagnetic micropulsations by using a large horizontal current loop on the ground. Most natural micropulsations appear to be produced by hydromagnetic (hm) waves propagating in the ionosphere and/or the magnetosphere, and the term "artificial micropulsations" is used to mean artificially-produced hm waves with propagation characteristics similar to those of the natural signals.

The critical quantity in the generation process for the hm waves is the amplitude of the magnetic field variation that can be produced in the ionospheric E-region by the ground-based loop. Currents are induced in the conducting earth beneath the loop whenever its current is varied, and these currents have a magnetic field opposing the magnetic field of the loop. If either the conductivity of the earth or the variation frequency is too high the field at E-region heights may be reduced to a level where negligible hm wave amplitudes are produced. The effect of these earth currents is calculated for an assumed single-layer earth and for a wide range of frequencies (10^{-2} - 10^2 Hz) and earth conductivities (10^{-5} - 4 mho/m). It is found that at 1 Hz and for a conductivity of 10^{-4} mho/m (representing a typical conductivity for the earth's crust) the magnetic field of the loop is reduced by about 18 percent. At lower frequencies the reduction in magnetic field is even less. Thus, provided the loop is suitably located, the effect of earth currents should not be very great.

Expressions for the two hm wave modes excited in the ionosphere by a current loop on the ground are derived and the feasibility of constructing large current loops is considered. It is concluded that current loops with magnetic moments as large as 7×10^{13} amp.m² are practicable and that the current in these loops can be varied at micropulsation frequencies. All things considered, the total magnetic field produced in the E-region could have an amplitude as large as 0.5 gamma, which is greater than most natural micropulsation amplitudes observed beneath the ionosphere.

Preliminary calculations with the expressions for the two hm wave modes indicate that significant hm wave amplitudes can be produced in the ionosphere above the larger current loops considered in this study. This conclusion is independently confirmed by Greifinger (1972). Thus, we conclude that the artificial generation of micropulsations is feasible and that a large current loop should be capable of producing observable Pc 1 micropulsations at very considerable distances (greater than 5000 km) from the source. Much further study is required to establish all the possibilities of the artificial generation process, particularly at low micropulsation frequencies and for field-line propagation. However, a number of important uses for artificially-generated micropulsations are immediately apparent and are discussed briefly.

CONTENTS

	<u>Page</u>
I. INTRODUCTION	1
A. Description of Micropulsations	1
B. Need for Artificial Generation	4
C. Plan of the Report	7
II. OUTLINE OF THE CURRENT LOOP METHOD FOR GENERATING MICROPULSATIONS.	9
A. Ineffectiveness of Current Loops in Free Space	9
B. Generation of Hyrdomagnetic Waves in the Ionosphere.	10
III. EFFECT OF INDUCED EARTH CURRENTS	15
A. Skin Depth	16
B. Field Induced by Current Loop.	21
1. Basic Equations.	21
2. Effect of the Earth.	27
3. Current Loop as Source	29
4. Numerical Solution of the Induced Field Equation	31
C. Conclusion	34
IV. GENERATION OF ALFVÉN WAVES IN THE IONOSPHERE	37
A. Coordinate Systems	37
B. Free Space Waves due to Current Loop	41
C. Alfvén Waves	43
D. Solution of the Boundary Value Problem	44
1. Fast Alfvén Wave	44
2. Slow Alfvén Wave	45
3. The Incident Wave.	46
4. The Perpendicular Reflected Wave	46
5. The Parallel Reflected Wave.	47
E. Booker Quartic	49
F. Determination of Field Components in the Unprimed Coordinate System.	50

	<u>Page</u>
G. Final Solution for the Fast Alfvén Wave.	51
H. Final Solution for the Slow Alfvén Wave.	53
V. SOME PRACTICAL CONSIDERATIONS.	55
A. Details of the Loop.	55
1. Construction	55
2. Size	57
3. Self-Inductance.	61
B. Power Management and Frequency Generation.	63
C. Location of the Current Loop	64
D. Cost of a Ground-Based Current Loop System	68
E. Environmental Aspects of Large Current Loops	68
VI. CONCLUSION	75
APPENDIX A. MAGNETIC FIELD OF A CURRENT LOOP IN FREE SPACE. . .	83
1. Dipole Expressions	83
2. Finite-Loop Expressions.	83
3. Comparison of the Dipole and Finite-Loop Fields. . . .	86
APPENDIX B. ALTERNATIVE EXPRESSIONS FOR THE TOTAL MAGNETIC FIELD PRODUCED BY A GROUND-BASED CURRENT LOOP . . .	87
APPENDIX C. FOURIER TRANSFORM OF LOOP CURRENT	91
REFERENCES.	95

TABLES

<u>Number</u>		<u>Page</u>
1.1	Micropulsation Nomenclature	1
3.1	Skin Depths for Certain Frequencies and Conductivities	17
3.2	Conductivities of Ice, Snow and Water.	18

ILLUSTRATIONS

<u>Figure</u>		<u>Page</u>
3.1	Cylindrical coordinate system for the current loop problem	20
3.2	Frequency variation of the maximum axial magnetic field produced by the 10 km loop (maximum current 1000 amps) at an altitude of 100 km. The parameter σ (mho/m) represents the conductivity of the earth, considered to be a single layer, and the dashed line indicates the field for a non-conducting earth	35
4.1	Model of the loop-ionosphere system.	38
4.2	Coordinate systems used in the calculation of the Alfvén waves excited in the ionosphere by the ground-based current loop. The z'' , k , and x'' axes all lie in one plane	39
5.1	Variation of the axial magnetic field at 100 km for a current loop of constant moment ($\pi \cdot 10^{11}$ amp.m ²) but variable radius.	58
5.2	Variation of the self-inductance of a single circular loop constructed of wire of gauge 2000 mcm (diameter ≈ 1.75 inches) as the loop radius is increased from ~ 0 km to 100 km	60
5.3	Block diagram of a power system for the 10 km loop . .	62
5.4	Surface resistivity of the United States (After Keller et al., 1966)	66

Figure

Page

5.5	Magnetic field variations in the planes of the two current loops discussed in the text. The field inside each of the loops is opposite to the field outside and its variation is indicated by a dashed line. For comparison, the equivalent dipole field variations are also shown.	70
C.1	Coordinate system for calculating the Fourier transform of the loop current.	92

ACKNOWLEDGMENT

We wish to thank Professor O. G. Villard, Jr., for his continued interest and many helpful suggestions during the course of this work. We also wish to thank Dr. Carl Greifinger for several stimulating conversations and Professor R. N. Bracewell for timely advice, early in this work, to "think big."

This work was supported by the Defense Advanced Research Projects Agency through the Office of Naval Research, Contract N00014-67-A-0112-0066.

I. INTRODUCTION

A. DESCRIPTION OF MICROPULSATIONS

Geomagnetic micropulsations are small approximately periodic fluctuations of the earth's magnetic field with periods in the range 0.2 - 600 seconds [see reviews by Jacobs (1970), Troitskaya (1967), or Campbell (1967)]. In the electromagnetic spectrum they constitute part of the ULF (ultra-low-frequency) band. There are a variety of naturally-occurring micropulsations and it is customary, following Jacobs et al (1964), to subdivide the micropulsations into two main classes according to whether they are "of a regular and mainly continuous character" (class Pc) or are characterized by "an irregular pattern" (class Pi). These two main classes of micropulsations are then further subdivided depending upon their period as shown in Table 1.1:

Table 1.1

Micropulsation Nomenclature

Notation	Period Range(sec.)	Notation	Period Range(sec.)
Pc 1	0.2 - 5	Pi 1	1 - 40
Pc 2	5 - 10	Pi 2	40 - 150
Pc 3	10 - 45		
Pc 4	45 - 150		
Pc 5	150 - 600		

The division into subgroups is based upon the physical and morphological properties of the micropulsations and thus classes Pc 1 and Pc 2, for example, represent (or are intended to represent) physically different micropulsations. This system of classification has been widely adopted by

micropulsation workers. It should be noted, however, that there are certain distinctive varieties of micropulsation activity that do not fit conveniently into the standard system of classification and have their own nomenclature. Probably the most important of these special varieties of micropulsations is the form of activity known as 'Intervals of Pulsations of Diminishing Period,' or IPDP's. These micropulsations were first defined by V. A. Troitskaya (Troitskaya, 1961) and they have become the subject of considerable research because of their occurrence during magnetospheric substorms [e.g. Carpenter et al, 1971, and references therein].

The properties of the various classes of micropulsations have been investigated rather thoroughly over the last decade, both on the ground and in space. It is now clear that micropulsations of all classes have their maximum amplitudes in the auroral zones. There is also a remarkable degree of correlation between micropulsations recorded at geomagnetically conjugate points. These are the major similarities. Most of the other properties of the micropulsations are found to differ markedly from one class to another.

An important distinguishing feature of the Pc 1 class of micropulsations is the presence of a fine frequency structure that is easily seen on their spectrograms (i.e. frequency-time displays). This frequency structure is absent from all other classes of Pc and Pi micropulsations. Scattered structural elements are sometimes observed during IPDP events, but they do not appear to be a primary characteristic of the micropulsations as they do with Pc 1. Detailed investigation of the frequency structure in Pc 1 micropulsations resulted in the present theory for their origin,

which is based upon a particular wave-particle interaction in the magnetosphere (e.g. Cornwall, 1965). It is not believed that wave-particle interactions play an important role in the origin of any of the other classes of Pc or Pi micropulsations.

Purely electromagnetic disturbances at micropulsation frequencies do not propagate in the ionospheric or magnetospheric plasma. The waves that do propagate involve both electromagnetic fields and periodic mass motions and they are strongly influenced by the ambient geomagnetic field; they are called hydromagnetic (hm) or magnetohydrodynamic (mhd) waves. There is an extensive literature concerning these important waves and their properties will not be discussed here in great detail. The reader is referred to the micropulsation review text by Jacobs (1970) for a relevant discussion. The properties of micropulsations, in particular their wide occurrence over the surface of the earth and similarity at conjugate locations, all point to an origin as hm waves in the ionosphere and above. Thus, when we refer to the artificial generation of micropulsations we are, strictly speaking, implying the generation of hm waves with micropulsation frequencies in the upper atmosphere. The surface effects of these hm waves, i.e., artificial geomagnetic micropulsations, occur when the hm waves reach the lower part of the ionospheric E-region and convert to electric currents. Magnetic fluctuations with a superficial similarity to natural micropulsations can be produced on the surface of the earth by various means (e.g., with a current loop) without intermediary hm waves. These disturbances are typically extremely localized and are physically distinct from micropulsations. We will not use the term artificial micropulsations for such fluctuations.

B. NEED FOR ARTIFICIAL GENERATION

Micro pulsation research has of necessity always involved the passive acquisition of data. Micropulsations are recorded as they occur naturally (and, in certain cases, infrequently) and the records are then processed to obtain information about the micropulsations. There has never been a wholly controlled method of generating micropulsations. High-altitude nuclear explosions, at present the only known method of artificial generation (e.g. Green et al., 1962; Crook et al., 1963; Bomke et al., 1964; Bowman and Mainstone, 1964; Kovach and Ben-Menahem, 1966), produce extremely noisy micropulsation signals in addition to having other obvious disadvantages. However, insofar as micropulsation studies are concerned, nuclear explosions have two very desirable characteristics. First, the source of the micropulsations is localized and, second, the generation of the micropulsations begins at a precisely known time. These characteristics enable propagation times to be calculated for the micropulsation disturbances, and thus information is obtained about the hydromagnetic waves that transmit the disturbances through the magnetosphere and ionosphere. Micropulsation propagation times are still of current interest (see Campbell and Thornberry, 1972), but measurements on the natural signals are at best difficult and tedious.

The limited usefulness of nuclear explosions for the generation of micropulsations suggests that a fully controlled method of generation could have a number of useful applications. (By fully controlled we mean that the frequency of the micropulsation source as well as its location, timing and power output are in principle all at the disposal of the experimenter).

This report is concerned with the possibility of using a very large current loop on the ground to generate hydromagnetic waves of micropulsation frequencies (i.e. micropulsations) in the overhead ionosphere. There are many advantages associated with this particular method of generation compared to other possible methods. Details of the current loop method of generation will be discussed in the next chapter. At this stage we will simply list some of the more important uses for an artificial source of micropulsations, such as may be provided by a large ground-based current loop:

1) Simple and direct studies of hydromagnetic wave propagation in the magnetosphere and ionosphere would become possible. Precise studies of the E-W and N-S propagation of Pc 1 micropulsations could be conducted for the first time. At lower frequencies it might be possible to excite resonances either along an entire field line or other specific sections of a field line (e.g. between the lower ionosphere and the Alfvén velocity maximum at ~3000 km altitude) (e.g. Jacobs and Watanabe, 1962; Fraser-Smith, 1967).

2) The cyclotron resonance interaction between electrons and VLF waves, and between protons and ULF waves, is of great current interest in magnetospheric studies. Energetic electrons (protons) may be precipitated out of the magnetosphere by VLF (ULF) wave injection, either natural or artificial, as a result of this interaction. The VLF and ULF waves, in turn, may be amplified through their interaction with the energetic particles.

At present there is little direct evidence for the cyclotron resonance interaction and its importance in the magnetosphere is largely inferred from

the properties of certain VLF and ULF wave phenomena and through the observation of limits on the fluxes of trapped charged particles. It is of interest that the interaction is thought to be essential for the generation and amplification of Pc 1 micropulsations (e.g. Cornwall, 1965; Liemohn, 1967).

Helliwell et al. (1972) recently reported some of the most direct evidence yet available for the interaction: the observation of VLF whistler-induced precipitation of energetic electrons. In addition, they noted the feasibility of conducting controlled experiments with a high-powered (100 kW) VLF transmitter at Siple Station in the Antarctic.

A large ground-based current loop would have a unique capability for experiments on the cyclotron resonance interaction at ULF frequencies, i.e. at frequencies much less than in the planned VLF experiments. In addition, the loop could precipitate energetic protons out of the magnetosphere and into the lower ionosphere on a semi-controlled basis. These protons would be useful in other experiments. Finally, the loop could be used to test experimentally the reality of the supposed Pc 1 micropulsation generation process.

3) Magnetotelluric studies of the crust and upper mantle would be facilitated. These studies are largely dependent upon naturally-occurring low frequency electromagnetic fluctuations on the earth's surface and there are many gaps in the available frequencies.

4) Provided sufficient power is available, as may be assumed for a ground-based generator, the ionosphere may be modified either by direct heating or by the generation of currents and hydromagnetic waves. In other words, studies of the ionosphere may be possible. At frequencies

above 1 Hz hydromagnetic waves are strongly absorbed in the ionosphere (e.g. Francis and Karplus, 1960; the location of the maximum of absorption varies with frequency) and there is an efficient conversion into heat of the energy deposited in the ionosphere. Unfortunately, the magnitude of the currents induced in the earth by the current loop also increases with frequency. These currents reduce the effectiveness of the loop and dissipate energy; they will be discussed in greater detail in Chapter III.

In addition to the above uses for an artificial, controlled source of micropulsations, there are less tangible benefits to be expected from a first attempt to conduct an experiment upon a natural system. Much has been surmised about the properties of the ionosphere and magnetosphere at micropulsation frequencies but there are very few definite experimental results. Both theoretical and experimental work would be stimulated by an attempt to generate artificial micropulsations, and there may be new discoveries. For example, the recent successful experiments to modify the ionosphere by using very high power HF radio transmissions (e.g. Utlaut, 1970; Carlson et al., 1972) produced some results that were completely unexpected and showed that the ionosphere, thought by many to be well-understood at HF frequencies, still had some novel properties that could not be easily explained.

C. PLAN OF THE REPORT

In Chapter II an outline is given of the suggested method of generation of micropulsations by using a large ground-based current loop. Chapters III and IV are concerned with the theory for two of the most important aspects of the generation process. In Chapter III

the effect of earth currents on the performance of the loop is calculated and in Chapter IV expressions are derived for the two forms of Alfvén wave produced by the loop in the ionosphere. Chapter III also contains a discussion of skin depths for selected materials comprising the earth's surface and crust. Some practical details of the loop are discussed in Chapter V and the overall conclusion of the report is given in Chapter VI. Three appendices contain subsidiary information required in the two theoretical chapters.

II. OUTLINE OF THE CURRENT LOOP METHOD FOR GENERATING MICROPULSATIONS

A. INEFFECTIVENESS OF CURRENT LOOPS IN FREE SPACE

Loop antennas have been used for many years to transmit and receive electromagnetic signals. In most cases these loops operate at frequencies in the upper kilohertz or megahertz range and their physical dimensions are small relative to the wavelengths involved, i.e., their radii do not exceed a few meters. Provided the loop dimensions are small compared to the wavelength of the transmitted signal, a loop antenna used as a transmitter is equivalent to a magnetic dipole with an oscillating moment. In calculating the fields radiated from such a dipole (e.g., Panofsky and Phillips, 1962) the wavelength λ of the radiation plays an important role in defining the radiation and induction zones. We will use the term "induction zone" to mean the region close to the dipole (transmitter) where the predominant electric and magnetic field components vary as r^{-2} or r^{-3} , with r indicating the distance from the dipole. Another term commonly used for the induction zone is "near-field region". The "radiation zone" starts at some distance from the dipole and extends to infinity. In this zone the electric and magnetic field components vary predominantly as r^{-1} . The transition region between the induction and radiation zones is not well-defined but it is approximately centered on the radial distance $r = \lambda$. Thus the fields are primarily inductive for distances less than a wavelength from the dipole and for distances greater than a wavelength they are primarily radiative. The importance of the wavelength as a scale factor now becomes apparent, because the inductive fields do not contribute to the radiated energy from the dipole.

These details become important when the fields generated by a large ground-based current loop are considered. For a 1 Hz frequency the wavelength of an electromagnetic wave in free space is 3×10^5 km, which is much larger than the radius of the earth (6370 km) and about an order of magnitude larger than the earth's circumference (4×10^4 km). Thus, for frequencies in the micropulsation range the direct magnetic field produced by a current loop is predominantly inductive at any point on the earth's surface. Close to the loop, i.e., within a few hundred kilometers, the induction magnetic field is simply the standard magnetic field for a current loop with an $e^{j\omega t}$ factor to allow for the time variation of the current in the loop. Expressions for the magnetic field produced by a steady current in a conducting loop are given in Appendix A, and it is shown that the field drops off as r^{-3} for distances r large compared to the loop radius. It is primarily for this reason that current loops in free space have been considered ineffective as generators of magnetic fluctuations at micropulsation frequencies: there is no significant radiation field and the magnetic field that is produced by the loop drops off too rapidly to be important at a distance.

B. GENERATION OF HYDROMAGNETIC WAVES IN THE IONOSPHERE

Although the magnetic field from a current loop drops off rapidly with distance, it is still possible for a large current loop on the ground to produce a magnetic field of the order of one gamma at the height of the ionospheric E-region (Details of such loops will be given in Chapter V). If the current in the loop is varied at a micropulsation frequency the E-region will experience a magnetic disturbance that is

large compared to most natural disturbances. It can be anticipated that the varying magnetic field will interact with the E-region plasma to produce hm waves. These waves then propagate away from the interaction region, possibly to large distances, either within the ionosphere or along the geomagnetic field. In general, artificial geomagnetic micropulsations will be produced on the ground wherever the hm waves are strong within the ionosphere, either through ionospheric ducting (Pc 1 frequencies; see Greifinger & Greifinger, 1968) or through propagation along the geomagnetic field lines (Pc 1 - Pc 5 frequencies; see Jacobs, 1970).

For ionospheric and magnetospheric plasmas, and micropulsation frequencies, there are just two modes of hm wave propagation that are of importance. These two modes are usually called "Alfvén" and "modified Alfvén" waves. Both modes can propagate at a general angle to the ambient magnetic field but, in contrast to the modified Alfvén waves, Alfvén waves tend to be strongly guided by the field. Also, the Alfvén waves do not propagate in a direction perpendicular to the ambient magnetic field, as do the modified Alfvén waves (when they are sometimes referred to as magnetosonic waves). The velocity of Alfvén waves along the magnetic field is the well-known Alfvén velocity V_A and is given by

$$V_A^2 = \frac{B_0^2}{\mu_0 \rho} \quad (2.1)$$

where B_0 is the steady magnetic field and ρ the plasma density. Two other terms commonly used for the Alfvén and modified Alfvén waves are "slow Alfvén" waves and "fast Alfvén" waves, respectively. This usage

reflects a difference in the phase velocities of the two waves. However, provided the wave frequencies are much less than the local ion gyro-frequency, there is little difference between the velocities of the fast and slow Alfvén waves in the ionosphere and magnetosphere. (The use of the term hydromagnetic usually implies that the wave frequencies ω are much less than the ion gyrofrequency of the plasma propagating the waves). We expect both hm modes to be excited by the current loop in the ionosphere, with the Alfvén mode propagating primarily in the direction of the geomagnetic field and the modified Alfvén mode propagating primarily within the ionosphere and becoming trapped in the F-region duct (Greifinger and Greifinger, 1968). Expressions for the two modes, as excited by a ground-based current loop, are derived in Chapter IV.

It should be emphasized that the current loop does not itself radiate artificial micropulsations. Instead, energy is fed into the E-region of the ionosphere by the alternating magnetic field of the loop. (The magnetic field does work upon the ionosphere). Hm waves then propagate away (radiate) from the interaction region to other parts of the ionosphere and magnetosphere, as described above. There is no significant radiation of micropulsation-frequency electromagnetic waves in the region between the earth and the ionosphere.

It will be quite easy experimentally to distinguish the artificial micropulsations generated by the current loop from the direct fluctuating magnetic field of the loop. The direct field can be calculated accurately and at moderate distances from the loop the magnetic field variation, with artificial micropulsations present, will be substantially larger than the calculated direct field variation. At large distances (≥ 1000 km; the

exact distance will depend on the loop magnetic moment and the sensitivity of the detection equipment) the direct field will be negligible and only artificial micropulsations will be observed together with any natural micropulsations that might be present. Conjugate point observations will also give direct verification of the generation process, because the direct field from the loop will probably be negligible at the conjugate point. Finally, if the current variations in the loop are coded, the artificial micropulsations (propagation velocity $\sim v_A$) will be delayed relative to the direct field from the loop (propagation velocity $\sim c$; i.e., the velocity of light in free space)..

The critical quantity in this proposed method for generating artificial micropulsations by using a ground-based current loop is the magnitude of the magnetic field that can be produced in the E-region. The magnitude of the magnetic field depends on only two factors: the magnetic moment of the loop and the conductivity of the earth. Of these two factors, the conductivity of the earth is the least capable of being controlled. The effect of currents induced in the conducting earth is discussed in the following chapter. There appears to be no fundamental problem in constructing current loops of large moment, and details of some suitable loops will be discussed in Chapter V. For practical reasons, the requirement for a large magnetic moment restricts consideration to current loops that are coplanar with the earth's surface.

III. EFFECT OF INDUCED EARTH CURRENTS

The effect of induced earth currents upon the micropulsation generating capability of the ground-based current loop is considered in this chapter. The induced currents are important because their magnetic field opposes the inducing magnetic field of the loop and the total magnetic field is everywhere smaller than it would be if the earth was a non-conductor. Since the effectiveness of the loop as a micropulsation generator depends upon the total field it produces at ionospheric heights, it can be seen that the presence of the conducting earth reduces the capability of the loop. Fortunately, the earth's surface is not everywhere composed of materials with a high conductivity, such as sea-water, and some important materials have very small conductivities. One of the major objectives of this chapter is to find how strongly the direct field of the loop is reduced by induced earth currents for a wide range of conductivities and frequencies.

The chapter starts with a definition of skin depth and a brief description of its variation for frequencies in the range 10^{-3} - 10^3 Hz and for some representative earth-surface conductivities. A complete analytic solution to the field equations is then presented for a system consisting of a current loop located on the surface of a single-layered earth. The plane of the loop is taken parallel to the surface of the earth. The final equation for the total field is solved numerically and graphs of the variation of total field with frequency and conductivity are plotted.

The particular theoretical approach used in this chapter is basically the same as that introduced by Price (1950) and later extended and modified

Preceding page blank

by various other authors, including Price (e.g., Gordon, 1951; Bhattacharyya, 1955; Price, 1962). There is also a very considerable literature concerned with related problems in magnetotelluric work (e.g., Wait, 1962; Mann, 1967; Ryu et al., 1970). It should be pointed out that there is a very different point of view between the magnetotelluric studies and the work reported here. This study is concerned with the effects produced by a ground-based current loop in the ionosphere, whereas the other studies are motivated largely by the possibility of sounding the structure of the earth. In the latter case it is the fields on the surface of the earth (i.e., the measured fields) that are of primary interest and the emphasis is on the behavior of the surface fields when the earth is multi-layered or has other structure, such as a discontinuity in the horizontal plane.

A. SKIN DEPTH

The skin depth δ is defined by the equation

$$\delta = \sqrt{\frac{2}{\mu_0 \omega \sigma}} \quad (3.0)$$

It provides a convenient measure of the depth of penetration of an electromagnetic field, varying with angular frequency ω , into a conductor of conductivity σ . Equation 3.0 is obtained by assuming that a plane electromagnetic wave is perpendicularly incident upon the surface of a plane conductor and then calculating the rate at which the electric field falls off with increasing depth in the conductor. The fall-off is exponential and the skin depth δ is the depth at which the amplitude of the electric field has fallen to $1/e$ of its value just inside the

surface of the conductor. The idealized conditions for the derivation of Equation 3.0 do not always apply in practical situations but the skin depth defined by the equation still provides a very useful indication of the depth of penetration of the fields.

Table 3.1

Skin Depths for Certain Frequencies and Conductivities

Frequency (Hz)	Conductivity (mho/meter)		
	10^{-4}	10^{-1}	4
10^{-3}	1590 km	50.3 km	7.95 km
10^{-2}	503 km	15.9 km	2.51 km
10^{-1}	159 km	5.03 km	795 m
1	50.3 km	1.59 km	251 m
10	15.9 km	503 m	79.5 m
45	7.50 km	237 m	37.5 m
10^2	5.03 km	159 m	25.1 m
10^3	1.59 km	50.3 m	7.95 m

Table 3.1 gives the skin depths for a number of frequencies and conductivities relevant to the present work. Sea water is easily the best conductor ($\sigma = 4$ mho/m) of the materials occurring in large quantities over the surface of the earth. A typical surface "earth" conductivity lies somewhere in the range $10^{-1} - 10^{-2}$ mho/m with the conduction caused largely by the presence of saline water. For certain dry rock and sand

formations the conductivity may fall below 10^{-4} mho/m. Pure ice and pure water have very low conductivities (of the order of 10^{-6} - 10^{-7} mho/m) but the conductivities observed in nature for ice and "pure" water vary widely depending upon the content of impurities, especially salt. Table 3.2, derived from data published by Evans (1965), lists some conductivities for ice, snow and water.

Table 3.2
Conductivities of Ice, Snow and Water

Material	Conductivity (mho/meter)
Pure Ice (-10°C)	10^{-7}
Glacial Ice, Alberta (0°C)	5×10^{-7}
Sea Ice (0.5% salinity; -7°C)	10^{-3}
Soft New Snow (-10°C)	10^{-9}
Compact Wet Snow (0°C)	10^{-6}
Pure Water	4×10^{-6}
Distilled Water	2×10^{-4}
Public Water Supply	10^{-3} - 5×10^{-2}
Sea Water	1 - 5

The earth's crust is generally considered to be about three miles thick (~ 5 km) under the sediments of the ocean floors and perhaps twenty miles thick (~ 30 km), on the average, under the continents. A layer of sedimentary rocks with a thickness varying from 0 - 5 km forms the upper

part of the continental crust. The sedimentary rocks are comparatively highly conducting, with conductivities in the range 10^{-4} - 10^{-1} mho/m as noted earlier. The magnitude and variation of the conductivity below the sedimentary layer has been, and still is, the subject of considerable debate. A good introduction is given by Mott and Biggs (1963). We will only comment that the comparatively cool granitic (upper) and basaltic (lower) materials comprising the major part of the crust have very low conductivities, possibly as low as 10^{-7} mho/m. The Mohorovičić discontinuity separates the crust from the asthenosphere, or upper part of the mantle. Below this discontinuity there is an increase in conductivity and it may reach values in excess of 10^{-2} mho/m.

A conductivity of 10^{-4} mho/m appears a reasonable estimate for the crust of the earth at continental locations where the sedimentary layers are either thin or of low conductivity. Table 3.1 shows that the varying magnetic field of the loop will easily penetrate the crust if the frequencies are about 1 Hz or less. For ~ 1 Hz fluctuations (i.e., Pc 1 micropulsations) it is probably still a good first order approximation that the earth is a single layer of conductivity 10^{-4} mho/m, but for frequencies less than about 0.2 Hz a two layer model would be more appropriate. The two layer profile of Cantwell and Madden (1960) for Massachusetts, consisting of an upper layer 70 km thick and of conductivity 1.2×10^{-4} mho/m above a basement layer of conductivity less than 1.2×10^{-1} mho/m, may then provide a good starting point.

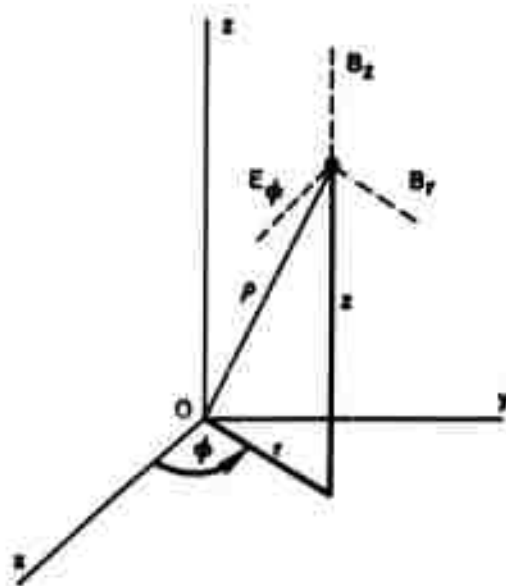


Figure 3.1 Cylindrical coordinate system for the current loop problem.

B. FIELD INDUCED BY A CURRENT LOOP

The field equations are now solved for a current loop source located above a single-layered conducting earth. The earth is represented by a semi-infinite homogeneous medium of uniform conductivity σ occupying the half-space $z < 0$ of a cylindrical coordinate system (r, ϕ, z) . The semi-infinite region above the earth ($z > 0$) is assumed to be free space (conductivity $\sigma = 0$, permittivity ϵ_0 , permeability μ_0). It is also assumed that the earth is non-magnetic, i.e., that the permeability is everywhere the same as that of free space. Initially, generality is maintained by specifying only that there is some field source at a height h above the surface of the earth ($z = 0$), that the z -axis passes through the source, and that there is rotational symmetry of the electromagnetic fields about the z -axis. In most previous work the field source is assumed to be a system of ionospheric currents and h is the height of the lower ionosphere. In the present work h will ultimately represent the height of the current loop above the ground, and the situation of most interest occurs when $h = 0$ and the loop is actually located on the ground.

1. Basic Equations

The following are the expressions for grad, div, curl and divgrad in cylindrical coordinates:

$$\text{grad } \psi = \frac{\partial \psi}{\partial r} \hat{r} + \frac{1}{r} \frac{\partial \psi}{\partial \phi} \hat{\phi} + \frac{\partial \psi}{\partial z} \hat{z} \quad (3.1)$$

$$\text{div } \underline{A} = \frac{1}{r} \frac{\partial(rA_r)}{\partial r} + \frac{1}{r} \frac{\partial A_\phi}{\partial \phi} + \frac{\partial A_z}{\partial z} \quad (3.2)$$

$$\text{curl } \underline{A} = \left[\frac{1}{r} \frac{\partial A_z}{\partial \phi} - \frac{\partial A_\phi}{\partial z} \right] \hat{r} + \left[\frac{\partial A_r}{\partial z} - \frac{\partial A_z}{\partial r} \right] \hat{\phi} + \frac{1}{r} \left[\frac{\partial(rA_\phi)}{\partial r} - \frac{\partial A_r}{\partial \phi} \right] \hat{z} \quad (3.3)$$

$$\text{divgrad } \Psi = \frac{1}{r} \frac{\partial}{\partial r} \left(r \frac{\partial \Psi}{\partial r} \right) + \frac{1}{r^2} \frac{\partial^2 \Psi}{\partial \phi^2} + \frac{\partial^2 \Psi}{\partial z^2} \quad (3.4)$$

where \hat{r} , $\hat{\phi}$, \hat{z} are unit vectors in the appropriate coordinate directions.

It is permissible at micropulsation frequencies to ignore the displacement current density $\dot{\underline{D}}$ and no generality is lost by assuming that the initial space-charge distribution is everywhere zero (Price, 1950). The field equations, in MKS units, are then

$$\text{div } \underline{D} = 0 \quad (3.5)$$

$$\text{div } \underline{B} = 0 \quad (3.6)$$

$$\text{curl } \underline{H} = \underline{J} \quad (3.7)$$

$$\text{curl } \underline{E} = -\dot{\underline{B}} \quad (3.8)$$

For the particular source considered in this problem there is rotational symmetry of the electromagnetic fields and it is easy to show that the components B_ϕ , E_r and E_z must all be zero. The magnetic and electric fields thus consist of the three components as follows

$$\underline{\tilde{B}} = (B_r, 0, B_z)$$

$$\underline{\tilde{E}} = (0, E_\phi, 0)$$

The coordinates and orientation of the field components are shown in Figure 3.1.

Solutions are now derived for the non-zero field components B_r , B_z and E_ϕ . (Because there is only one component of electric field the subscript ϕ will be dropped from E_ϕ). The time variation of the electric and magnetic fields is taken to be sinusoidal of angular frequency ω and

$$|\underline{\tilde{B}}| = \text{Re} \left\{ B e^{j\omega t} \right\}$$

$$|\underline{\tilde{E}}| = \text{Re} \left\{ E e^{j\omega t} \right\}$$

where the amplitudes E and B are functions of position only.

Initially, consider the fields within the conducting medium. Equations (3.7) and (3.8) give

$$E = \frac{1}{\sigma} \left(\frac{\partial H_r}{\partial z} - \frac{\partial H_z}{\partial r} \right) \quad (3.9)$$

$$B_r = \frac{1}{j\omega} \frac{\partial E}{\partial z} \quad (3.10)$$

$$B_z = -\frac{1}{j\omega} \left(\frac{\partial E}{\partial r} + \frac{E}{r} \right) \quad (3.11)$$

Combining these equations gives

$$\frac{\partial^2 E}{\partial z^2} + \frac{\partial^2 E}{\partial r^2} + \frac{1}{r} \frac{\partial E}{\partial r} - \left[\frac{1}{r^2} + j\omega\mu_0\sigma \right] E = 0 \quad (3.12)$$

where $\omega\mu_0\sigma$ is twice the inverse square of the skin depth.

Solutions to (3.12) are obtained by the method of separation of variables. Let

$$E = R(r) Z(z) \quad (3.13)$$

Substituting (3.13) in (3.12) gives

$$\left(\frac{1}{Z} \frac{d^2 Z}{dz^2} - j\omega\mu_0\sigma \right) + \left(\frac{1}{R} \frac{d^2 R}{dr^2} + \frac{1}{Rr} \frac{dR}{dr} - \frac{1}{r^2} \right) = 0$$

Because the quantities in parentheses are independent it follows that

$$\frac{d^2 R}{dr^2} + \frac{1}{r} \frac{dR}{dr} + \left[\lambda^2 - \frac{1}{r^2} \right] R = 0 \quad (3.14)$$

$$\frac{d^2 Z}{dz^2} - (\lambda^2 + j\omega\mu_0\sigma) Z = 0 \quad (3.15)$$

where $-\lambda^2$ is the separation constant and where the $\omega\mu_0\sigma$ is twice the inverse square of the skin depth.

Equation (3.14) may be written in the form

$$\frac{d^2 R}{d(\lambda r)^2} + \frac{1}{(\lambda r)} \frac{dR}{d(\lambda r)} + \left(1 - \frac{1}{(\lambda r)^2} \right) R = 0 \quad (3.16)$$

which is a form of Bessel's equation with solutions

$$R(r) = J_1(\lambda r) \quad (3.17)$$

i.e., Bessel's functions of the first kind, of order 1.

There are two solutions to equation (3.15). For $0 < z < h$, i.e., in free space, $\sigma = 0$ and

$$Z = C_1 e^{\lambda z} + C_2 e^{-\lambda z} \quad (3.18)$$

For $z < 0$, i.e., within the earth, it is only possible to specify solutions $Z(z, \lambda)$ that vanish at infinity.

Thus,

$$E_- = Z(z, \lambda) J_1(\lambda r) \quad z < 0$$

$$E_+ = (C_1 e^{\lambda z} + C_2 e^{-\lambda z}) J_1(\lambda r) \quad 0 < z < h \quad (3.19)$$

The standard boundary conditions for the interface at $z = 0$ reduce to the conditions that E , B_r and B_z should all be continuous across the boundary. Application of these conditions gives

$$Z(0, \lambda) = C_1 + C_2 \quad (3.20)$$

$$\left[\frac{\partial Z}{\partial z} \right]_{z=0} = \lambda(C_1 - C_2) \quad (3.21)$$

By using (3.20) and (3.21) and the relationship

$$J_1'(x) = J_0(x) - \frac{1}{x} J_1(x)$$

two equations for the magnetic field components in the region $h > z > 0$ are obtained, i.e.,

$$B_r = + \frac{\lambda}{j\omega} (C_1 e^{\lambda z} - C_2 e^{-\lambda z}) J_1(\lambda r) \quad (3.22)$$

$$B_z = - \frac{\lambda}{j\omega} (C_1 e^{\lambda z} + C_2 e^{-\lambda z}) J_0(\lambda r) \quad (3.23)$$

Also, since

$$J_0'(x) = -J_1(x),$$

Equations (3.22) and (3.23) can be written in the alternate form

$$B_r = \frac{\partial}{\partial r} \left[- \frac{J_0(\lambda r)}{j\omega} (C_1 e^{\lambda z} - C_2 e^{-\lambda z}) \right] \quad (3.24)$$

$$B_z = \frac{\partial}{\partial z} \left[- \frac{J_0(\lambda r)}{j\omega} (C_1 e^{\lambda z} - C_2 e^{-\lambda z}) \right] \quad (3.25)$$

In free space $\text{curl } \underline{\underline{B}} = 0$ and a magnetic scalar potential Ω may be defined by the equation

$$\underline{\underline{B}} = - \mu_0 \text{grad } \Omega \quad (3.26)$$

Equations (3.24) and (3.25) show that in this problem the magnetic scalar potential in the region $0 < z < h$ is of the form

$$\Omega = \frac{J_0(\lambda r)}{j\omega\mu_0} (C_1 e^{\lambda z} - C_2 e^{-\lambda z}) \quad (3.27)$$

The part of Ω that involves $e^{\lambda z}$ increases with z (in the indicated region) and may be identified with the inducing field, while the part involving $e^{-\lambda z}$ represents the field due to induced currents in the conducting region (e.g., Price, 1950, 1962; Battacharyya, 1955; Weaver, 1964). The induced field is finally found by expressing C_2 and $Z(z, \lambda)$ in terms of C_1 , which is assumed to be known. The present problem is not directly concerned with the induced field within the conductor. However, it is still necessary to consider the $Z(z, \lambda)$ solutions in some detail in order to relate C_2 to C_1 . The appropriate form of C_1 for a current loop source must also be found or, equivalently, the inducing potential must be expressed in the form of a sum (or integral) of terms of the type $Ce^{\lambda z} J_0(\lambda r)$.

2. Effect of the Earth

The solutions $Z(z, \lambda)$ to Equation (3.15) will now be considered in greater detail. The equation may be written

$$\frac{d^2 Z}{dz^2} - \theta^2 Z = 0 \quad (3.28)$$

where

$$\theta^2 = \lambda^2 + j\omega\mu_0\sigma \quad (3.29)$$

and Equation (3.28) has solutions

$$Z(z, \lambda) = Fe^{\theta z} + Ge^{-\theta z} .$$

However, it is necessary that $Z(z, \lambda) \rightarrow 0$ as $Z \rightarrow -\infty$. Thus $G = 0$ and

$$Z(z, \lambda) = Fe^{\theta z} \quad (z < 0) . \quad (3.30)$$

Applying the boundary conditions, i.e., using equations (3.20) and (3.21), we obtain

$$F = C_1 + C_2$$

and

$$\theta F = \lambda(C_1 - C_2)$$

or

$$C_2 = -\frac{(\theta-\lambda)}{(\theta+\lambda)} C_1 . \quad (3.31)$$

Thus, outside the earth ($0 < z < h$) the magnetic scalar potential of the induced magnetic field is given by

$$\Omega_i = - \frac{(\theta - \lambda)}{(\theta + \lambda)} C_1 e^{-\lambda z} J_0(\lambda r) \quad (3.32)$$

3. Current Loop as Source

The current loop dimensions considered in this report are mostly small compared to the earth-ionosphere distance and a dipole approach is adequate for calculation of the electromagnetic fields. A plane current loop carrying current I and of infinitesimal area dS has a magnetic dipole moment M , where

$$M = I dS \quad (3.33)$$

In free space the magnetic scalar potential for such a dipole is given by

$$\Omega_d = \frac{M}{4\pi} \frac{(z - h)}{[r^2 + (z - h)^2]^{3/2}} \quad (3.34)$$

where the dipole is located at $z = +h$ on the z axis of a cylindrical system of coordinates and has its axis aligned along the (positive) z direction. Equation (3.34) can be written

$$\Omega_d = - \frac{M}{4\pi} \frac{\partial}{\partial z} \left(\frac{1}{\rho} \right) \quad (3.35)$$

where $\rho = [r^2 + (z - h)^2]^{1/2}$ is the radial distance from the dipole to the field point. The following formula (Sneddon, 1955)

$$\int_0^{\infty} J_0(\lambda r) e^{\lambda(z-h)} d\lambda = \frac{1}{\rho} \quad (z < h) \quad (3.36)$$

may be used to write (3.35) in the form

$$\Omega_d = -\frac{M}{4\pi} \int_0^{\infty} J_0(\lambda r) e^{\lambda(z-h)} \lambda d\lambda \quad (z < h) \quad (3.37)$$

For a dipole at the origin, and $z > 0$,

$$\begin{aligned} \Omega_d &= \frac{M}{4\pi} \int_0^{\infty} J_0(\lambda r) e^{-\lambda z} \lambda d\lambda \\ B_r &= \frac{\mu_0 M}{4\pi} \int_0^{\infty} J_1(\lambda r) e^{-\lambda z} \lambda^2 d\lambda \\ B_z &= \frac{\mu_0 M}{4\pi} \int_0^{\infty} J_0(\lambda r) e^{-\lambda z} \lambda^2 d\lambda \end{aligned} \quad (3.38)$$

The negative sign in equation (3.37) comes from the assumption that the magnetic dipole moment is directed in the positive z direction. The dipole moment is actually oscillatory ($I = I_0 e^{j\omega t}$) and the sign is not really significant.

The potential given by equation (3.37) satisfies the requirements previously discussed for a suitable inducing potential. Combining (3.37) and (3.32) the following equation for the induced field in the region $z > 0$ is obtained

$$\Omega_1 = \frac{M_0}{4\pi} \int_0^{\infty} \frac{\theta-\lambda}{\theta+\lambda} e^{-\lambda(z+h)} J_0(\lambda r) \lambda d\lambda \quad (3.39)$$

where $M_0 = I_0 dS$. Thus, for the dipole (loop) at the origin of coordinates, the induced field in the region $z > 0$ is given by

$$\Omega_1 = \frac{M_0}{4\pi} \int_0^{\infty} \frac{\theta-\lambda}{\theta+\lambda} e^{-\lambda z} J_0(\lambda r) \lambda d\lambda \quad (3.40)$$

Equations (3.39) and (3.40) represent the formal solution to our problem.

4. Numerical Solution of the Induced Field Equation

We now concentrate upon Equation (3.40) for the induced field produced by an infinitesimal current loop placed upon the earth's surface. The integral in this equation was solved analytically by Gordon (1951), but unfortunately the solutions so obtained are unwieldy and limited in their application. We chose to evaluate the integral numerically by using one of the integration routines available for Stanford's IBM 360/67 computer. First, however, it was necessary to derive a suitable expression for the real part of the induced field equations. Equations (3.40) and (3.26) give the following two equations for the induced magnetic field components:

$$\begin{aligned} B_r &= \frac{\mu_0 M_0}{4\pi} \int_0^{\infty} \frac{\theta-\lambda}{\theta+\lambda} e^{-\lambda z} J_1(\lambda r) \lambda^2 d\lambda \\ B_z &= \frac{\mu_0 M_0}{4\pi} \int_0^{\infty} \frac{\theta-\lambda}{\theta+\lambda} e^{-\lambda z} J_0(\lambda r) \lambda^2 d\lambda \end{aligned} \quad (3.41)$$

Note that for $r = 0$ (i.e. on the z axis) we have $J_1(0) = 0$ and $J_0(0) = 1$.

Thus, $B_r = 0$ as required and

$$\begin{aligned} \Omega \text{ (axis)} &= \frac{M_0}{4\pi} \int_0^\infty \frac{\theta - \lambda}{\theta + \lambda} e^{-\lambda z} \lambda d\lambda \\ B_z \text{ (axis)} &= \frac{M_0}{4\pi} \int_0^\infty \frac{\theta - \lambda}{\theta + \lambda} e^{-\lambda z} \lambda^2 d\lambda \end{aligned} \quad (3.42)$$

The solution of the equation for B_z (axis) will enable us to compare the direct field from the loop with the induced field in the most important region of the ionosphere for the production of hydromagnetic waves, i.e., in the E-region directly above the loop.

Let

$$\theta = a + jb = (\lambda^2 + j\omega\mu_0\sigma)^{1/2} \quad (3.43)$$

where both a and b are real. Solving for a and b , we obtain

$$\begin{aligned} a &= 2^{-1/2} [\lambda^2 + (\lambda^4 + \omega^2 \mu_0^2 \sigma^2)^{1/2}]^{1/2} \\ b &= 2^{-1/2} [-\lambda^2 + (\lambda^4 + \omega^2 \mu_0^2 \sigma^2)^{1/2}]^{1/2} \end{aligned} \quad (3.44)$$

The real part of equations (3.41) are separated out by writing

$$\begin{aligned} \frac{\theta - \lambda}{\theta + \lambda} &= \frac{(a - \lambda) + jb}{(a + \lambda) + jb} \\ &= \frac{a^2 + b^2 - \lambda^2}{(a + \lambda)^2 + b^2} + j \frac{2\lambda b}{(a + \lambda)^2 + b^2} \end{aligned}$$

Thus, we obtain the final expressions for B_r and B_z :

$$B_r \text{ (real)} = \frac{\mu_0 M_0}{4\pi} \int_0^{\infty} \left[\frac{a^2 + b^2 - \lambda^2}{(a+\lambda)^2 + b^2} \right] e^{-\lambda z} J_0(\lambda r) \lambda^2 d\lambda$$

$$B_z \text{ (real)} = \frac{\mu_0 M_0}{4\pi} \int_0^{\infty} \left[\frac{a^2 + b^2 - \lambda^2}{(a+\lambda)^2 + b^2} \right] e^{-\lambda z} J_1(\lambda r) \lambda^2 d\lambda$$
(3.45)

with the auxiliary quantities a and b defined by equations (3.44).

Note that as $\sigma \rightarrow 0$ both B_z (real) and B_r (real) also tend to zero, and as $\sigma \rightarrow \infty$ we obtain simple dipole expressions. In other words, the induced fields given by equations (3.45) vary in the required manner.

The integral in the equation for B_z (real) with $r = 0$ (i.e., axial values) was integrated numerically for frequencies in the range 10^{-2} - 100 Hz and conductivities in the range 10^{-5} - 4 mho/m. Other data used in the computation were $z = 100$ km and $M_0 = \pi \cdot 10^{11}$ amp. m². These latter values correspond to a field point at E-region height and a loop of 10 km radius carrying a current of 1000 amp. With no contribution from the earth the magnitude of the B_z field at the field point would be 62.83 mγ (see Appendix A).

Figure 3.2 summarizes the results obtained from the numerical integration. The total B_z field is plotted in the figure and each curve shows the variation of the total field with frequency for a particular value of the earth conductivity. The dashed line indicates the "ideal" or zero earth conductivity magnitude of the field. It can be seen that for a good conductor such as sea-water ($\sigma = 4$ mho/m) the total field is very much less than the ideal value; at 1 Hz the total field is less than

one percent of the zero conductivity field. However, for conductivities typical of the solid earth the reduction of the dipole field by the induced field is not nearly so marked. For a conductivity of 10^{-4} mho/m, which we consider typical of some regions of the earth, the total field is 51.4 mγ for a frequency of 1 Hz. This value is only about 18 percent smaller than the zero conductivity field.

At higher frequencies, and especially for the greater conductivities, the curves in Figure 3.2 become straight lines. In fact, as shown in Appendix B, when $z \gg$ skin depth the total field becomes proportional to $(\omega\sigma)^{-1/2}$. When the conditions for this approximation apply, and for the data used to prepare Figure 3.2, the B_z field may be written

$$B_z(\text{total}) = \frac{2.37}{(\omega\sigma)^{1/2}} \text{ m}\gamma \quad (z > \text{skin depth}) \quad . \quad (3.46)$$

This equation, or the more explicit form in Appendix B, may be useful under some circumstances. However, it is only very approximate for the frequencies (~ 1 Hz) and conductivities ($\sim 10^{-4}$ mho/m) that are of particular interest in this report.

C. CONCLUSION

The results presented in this chapter enable us to reach an important conclusion about the probable effect of induced earth currents on the micropulsation generating capability of the ground-based current loop. Provided some care is taken in choosing the location of the loop, it appears likely that the magnetic field produced by the earth currents will remain considerably smaller than the direct field of the loop. For a

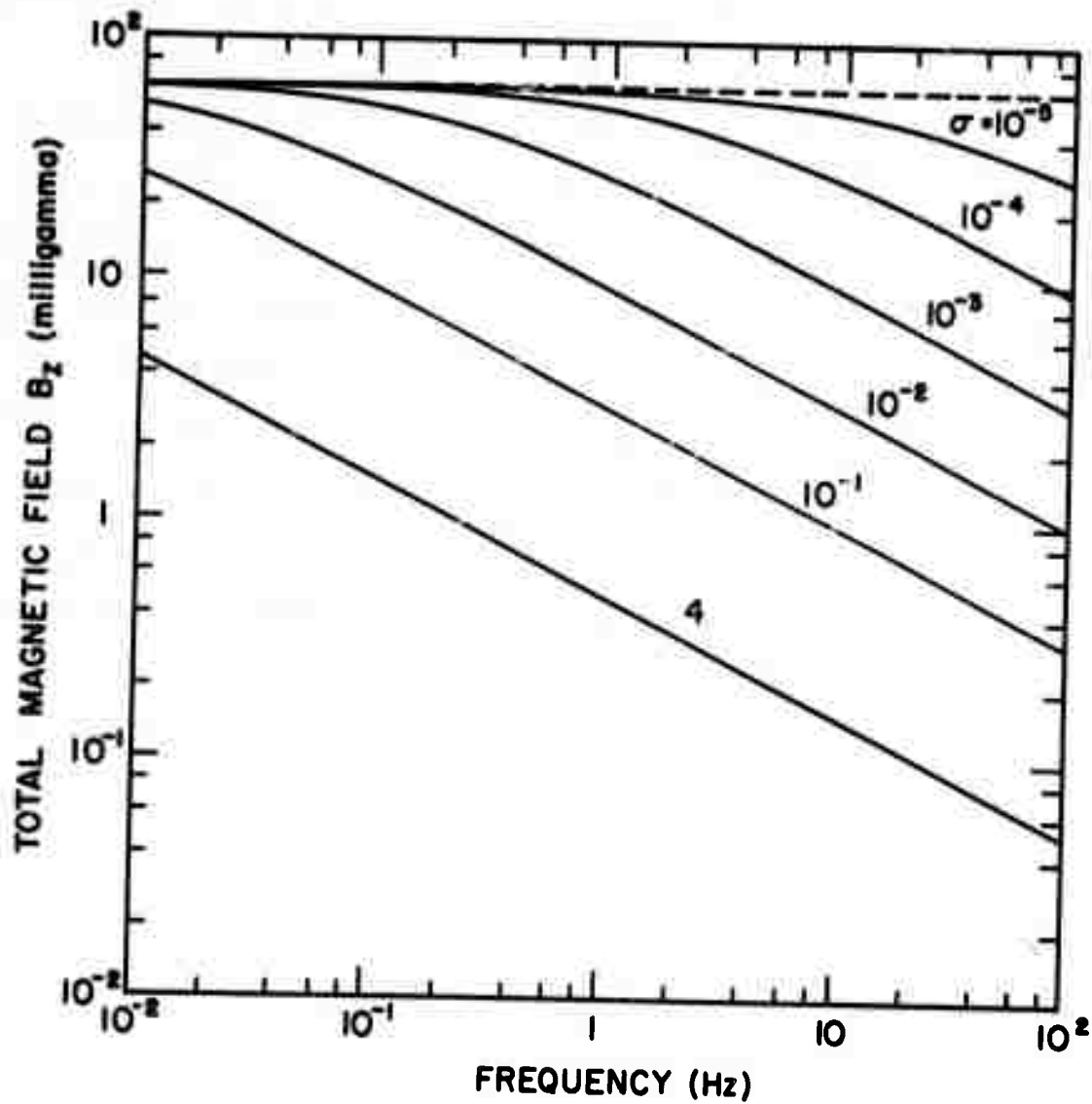


Figure 3.2. Frequency variation of the maximum axial magnetic field produced by the 10 km loop (maximum current 1000 amps) at an altitude of 100 km. The parameter σ (mho/m) represents the conductivity of the earth, considered to be a single layer, and the dashed line indicates the field for a non-conducting earth.

frequency of 1 Hz, if the loop is located on a reasonably non-conducting surface material ($\sigma \approx 10^{-3} - 10^{-4}$ mho/m in the first 1-5 km of crust), it is probable that the magnetic field of the loop at E-region heights will not be reduced by more than 20 percent from its zero earth conductivity value.

A more extended calculation of the effect of induced earth currents is desirable but it is unlikely to affect the above conclusion to any significant extent. A more realistic model of the earth's structure would primarily require the addition of a deep layer of higher conductivity than 10^{-4} mho/m. The addition of this deep layer would produce its greatest effect at the low frequencies (less than 1 Hz) where the skin depth is comparatively large. However, the curves in Figure 3.2 show that the magnetic field of the loop at low frequencies is negligibly affected by the upper layer of conductivity 10^{-4} mho/m and the depth of the more-conducting layer will necessarily minimize the field of its induced currents at ionospheric heights (the field from the induced currents probably drops off approximately as the inverse cube of the distance to the field point).

IV. GENERATION OF ALFVÉN WAVES IN THE IONOSPHERE

In this chapter we derive expressions for the Alfvén waves excited in the ionosphere by a current loop on the ground. In order to use Fourier techniques we utilize the model shown in Figure 4.1 consisting of two adjoining semi-infinite homogeneous regions permeated by a constant magnetic field, B_0 . The lower region is free space and contains the current loop, while the upper region is a plasma and supports the propagation of Alfvén waves.

A. COORDINATE SYSTEMS

Three separate coordinate systems, shown in Figure 4.2, are used to study the waves associated with the problem. The (x, y, z) system is chosen so that the z -axis points in the vertical direction and B_0 lies in the (x, z) plane. The (x', y', z') system is chosen so that z and z' coincide and so that k lies in the (x', z') plane. A third coordinate system, (x'', y'', z'') is chosen so that B_0 points in the z'' direction and k lies in the (x'', z'') plane. B_0 and k can be written in these systems as

$$\begin{aligned} \underline{B}_0 &= B_0 (\sin \varphi \underline{i}_x + \cos \varphi \underline{i}_z) \\ &= B_0 (\underline{l}'_x + \underline{m}'_y + \underline{n}'_z) \\ &= B_0 \underline{i}''_z \end{aligned} \tag{4.1}$$

$$\begin{aligned} \underline{k} &= k_x \underline{i}_x + k_y \underline{i}_y + k_z \underline{i}_z = k (\sin \theta \underline{i}'_x + \cos \theta \underline{i}'_z) \\ &= k (\sin \Psi \underline{i}''_x + \cos \Psi \underline{i}''_z) \end{aligned} \tag{4.2}$$

where $\underline{i}_x, \underline{i}_y$, etc. are unit vectors.

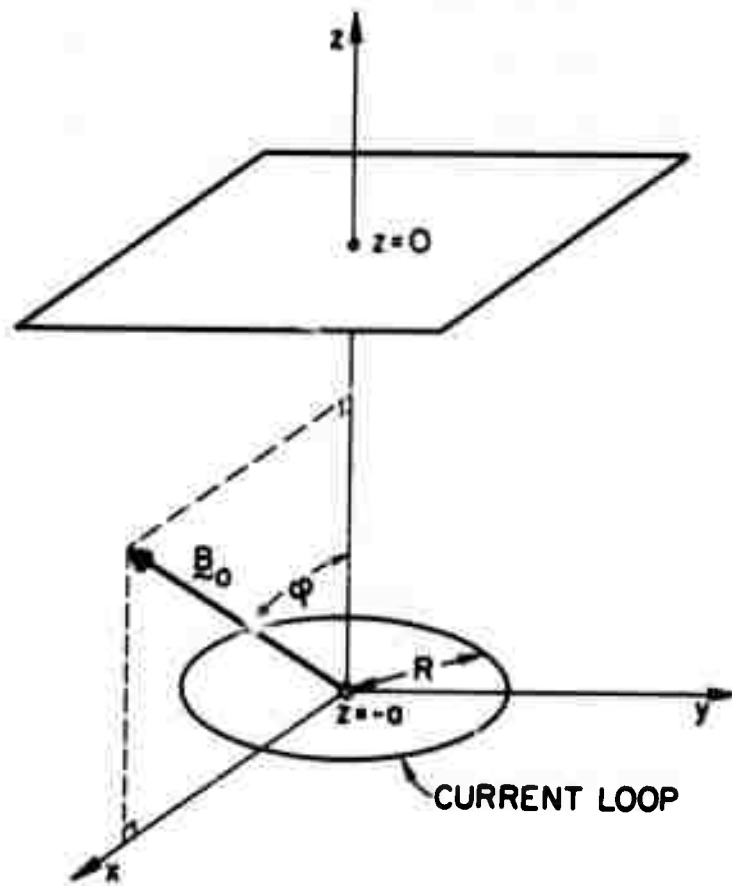


Figure 4.1 Model of the loop-ionosphere system.

The primed and unprimed coordinate systems are related by the transformation

$$\tilde{r} = \begin{vmatrix} \frac{k_x}{k_\perp} & \frac{k_y}{k_\perp} & 0 \\ \frac{k_y}{k_\perp} & \frac{k_x}{k_\perp} & 0 \\ 0 & 0 & 1 \end{vmatrix} \tilde{r}' \quad (4.3)$$

where $k_\perp = (k_x^2 + k_y^2)^{1/2}$

Furthermore, it can be shown that the primed and double-primed coordinate systems are related by the transformation

$$\tilde{r}' = \begin{vmatrix} \frac{\sin \Theta(1-l^2) - ln \cos \Theta}{\sin \Psi} & \frac{m \cos \Theta}{\sin \Psi} & l \\ -m \cot \Psi & \frac{n \sin \Theta - l \cos \Theta}{\sin \Psi} & m \\ \frac{\cos \Theta(1-n^2) - ln \cos \Theta}{\sin \Psi} & -\frac{m \sin \Theta}{\sin \Psi} & n \end{vmatrix} \tilde{r}'' \quad (4.4)$$

By reference to Figure 4.2, it can also be demonstrated that

$$l = \frac{k_x}{k_\perp} \sin \varphi \quad m = \frac{-k_y}{k_\perp} \sin \varphi \quad n = \cos \varphi \quad (4.5)$$

$$\sin \Theta = k_\perp/k \quad (4.6)$$

$$\cos \Psi = l \sin \Theta + n \cos \Theta = \frac{k_x \sin \varphi \sin \Theta}{k_\perp} + \cos \Theta \cos \varphi \quad (4.7)$$

B. FREE SPACE WAVES DUE TO CURRENT LOOP

The governing equations in free space are

$$\nabla \times \underline{E} = -j\omega\mu_0 \underline{H} \quad (4.8)$$

$$\nabla \times \underline{H} = j\omega\epsilon_0 \underline{E} + \underline{J} \quad (4.9)$$

Their Fourier transform is given by

$$\underline{k} \times \underline{E}_k = \omega\mu_0 \underline{H}_k \quad (4.10)$$

$$-j\underline{k} \times \underline{H}_k = j\omega\epsilon_0 \underline{E}_k + \underline{J}_k \quad (4.11)$$

or, upon elimination of \underline{E}_k , by

$$\underline{k}(\underline{k} \cdot \underline{E}_k) - k^2 \underline{E}_k + k_0^2 \underline{E}_k = j\omega\mu_0 \underline{J}_k \quad (4.12)$$

$$\text{where } k_0^2 = \frac{\omega^2}{c^2} \quad (4.13)$$

Taking the scalar product of this equation with \underline{k} gives

$$\underline{k} \cdot \underline{E}_k = j\omega\mu_0 \frac{\underline{k} \cdot \underline{J}_k}{k_0^2} \quad (4.14)$$

and, finally,

$$\underline{E}_k = - \frac{j\omega\mu_0 (k_0^2 \underline{J}_k - \underline{k}(\underline{k} \cdot \underline{J}_k))}{k_0^2 (k^2 - k_0^2)} \quad (4.15)$$

In Appendix C it is shown that

$$\underline{J}_k = \frac{-j}{8\pi} \underline{k} \times \underline{M} \exp(-jk_z a) \quad (4.16)$$

where \underline{M} is the vector magnetic moment of the current loop. Therefore \underline{E}_k in equation (4.15) becomes

$$\underline{E}_k = - \frac{\omega\mu_0}{8\pi} \frac{\underline{k} \times \underline{M}}{k^2 - k_0^2} \exp[-jk_z a] \quad (4.17)$$

Taking the inverse transform with respect to z gives

$$\underline{E}(k_x, k_y, z) = - \int_{-\infty}^{\infty} \frac{j\omega\mu_0 k_x M}{8\pi^2 k^2 - k_0^2} \exp[-jk_z(z+a)] dk_z \quad (4.18)$$

Performing the usual contour integration gives

$$\underline{E}(k_x, k_y, z) = \frac{j\omega\mu_0 k_x M \exp[-jk_{z0}(z+a)]}{8\pi^2 k_{z0}} \quad (4.19)$$

where $k_{z0} = \sqrt{k_0^2 - k_x^2}$ (4.20)

For future reference, note that this may be written in the primed coordinate system as

$$\underline{E} = E'_{yI} \exp[-jk_{z0}(z+a)] \underline{i}'_y \quad (4.21)$$

where

$$E'_{yI} = - \frac{-jk_x \omega\mu_0 M}{8\pi^2 k_{z0}} \quad (4.22)$$

C. ALFVÉN WAVES

The theory for Alfvén waves is well documented and only the results will be quoted here (Clemmow and Dougherty, 1969). The fast wave obeys the dispersion relation

$$\left(\frac{kc}{\omega}\right)^2 = L_1 \quad (4.23)$$

where

$$L_1 = 1 + \left(\frac{c}{V_A}\right)^2 \quad V_A = \frac{B_0}{[\mu_0 N(m_e + m_i)]^{1/2}} \quad (4.24)$$

V_A is the Alfvén velocity, m_e and m_i are the electron and ion mass, and N is the equilibrium number density. Referring to Figure 4.2, the electric field is linearly polarized in the y'' direction, i.e., $\underline{E} = E'' \underline{i}_y''$

The slow wave obeys the dispersion relation

$$\left(\frac{kc}{\omega}\right)^2 = \frac{L_1 L_0}{L_0 \cos^2 \Psi + L_1 \sin^2 \Psi} \quad (4.25)$$

where

$$L_0 = 1 - \frac{\omega_{pe}^2}{\omega^2} \approx -\frac{\omega_{pe}^2}{\omega^2} \quad (4.26)$$

and ω_{pe} is the plasma frequency.

The H-field is linearly polarized in the y'' -direction and the E-field is elliptically polarized in the (x, z) plane such that

$$E''_x = \frac{k \cos \Psi}{\omega \epsilon_0 L_1} H''_y, \quad E''_z = \frac{-k \sin \Psi}{\omega \epsilon_0 L_0} H''_y. \quad (4.27)$$

D. SOLUTION OF THE BOUNDARY VALUE PROBLEM

When each plane wave generated by the current loop strikes the boundary with the plasma, two plane waves are reflected back into free space and fast and slow Alfvén waves are transmitted into the plasma. In this section the amplitudes of the Alfvén waves are calculated.

1. Fast Alfvén Wave

We now consider the fast and slow Alfvén waves and designate quantities relative to them with subscripts a and b, respectively. The fast wave has only one component E''_{ya} in the double primed system, and therefore, using Eq. 4.4, its electric field components in the primed system are given by

$$E'_{xa} = \frac{m \cos \theta}{\sin \psi_a} E''_{ya} \quad (4.28)$$

$$E'_{ya} = \frac{n \sin \theta_a - l \cos \theta_a}{\sin \psi_a} E''_{ya} \quad (4.29)$$

$$E'_{za} = - \frac{m \sin \theta_a}{\sin \psi_a} E''_{ya} \quad (4.30)$$

The H-field components are found from the equation

$$\vec{H}'_a = \frac{1}{\omega \mu_0} \vec{k}_a \times \vec{E}'_a = \frac{k}{\omega \mu_0} (\sin \theta_a, 0, \cos \theta_a) \times (E'_{xa}, E'_{ya}, E'_{za}) \quad (4.31)$$

to be given by

$$H'_{xa} = \frac{k_a}{\omega \mu_0} \cos \theta_a [n \sin \theta_a - l \cos \theta_a] E''_{ya} \quad (4.32)$$

$$H'_{ya} = \frac{k_a}{\omega \mu_0} \frac{m}{G_a} E''_{ya} \quad (4.33)$$

$$H'_{za} = \frac{k_a}{\omega \mu_0} \sin \theta_a \frac{n \sin \theta_a - l \cos \theta_a}{G_a} E''_{ya} \quad (4.34)$$

2. Slow Alfvén Wave

Now consider the slow wave. Since there is only one component of \underline{H}_b in the double-primed coordinate system, H''_{by} , we find from Eq. (4.4) that the H-field in the primed system is given by

$$H'_{xb} = \frac{m \cos \theta_b}{\sin \psi_b} H''_{yb} \quad (4.35)$$

$$H'_{yb} = \frac{n \sin \theta_b - l \cos \theta_b}{\sin \psi_b} H''_{yb} \quad (4.36)$$

$$H'_{zb} = - \frac{m \sin \theta_b}{\sin \psi_b} H''_{yb} \quad (4.37)$$

Likewise, upon substituting Eqs. (4.27) into Eq. (4.4), we obtain

$$E'_{xb} = \left(\frac{k \cos \psi_b \sin \theta_b}{\omega \epsilon_0 L_1 \sin \psi_b} - \frac{l \omega \mu_0}{k \sin \psi_b} \right) H''_{yb} \quad (4.38)$$

$$E'_{yb} = - \frac{n \omega \mu_0}{k \sin \psi_b} H''_{yb} \quad (4.39)$$

$$E'_{zb} = \left(\frac{k \cos \psi_b \cos \theta_b}{\omega \epsilon_0 L_0 \sin \psi_b} - \frac{n \omega \mu_0}{k \sin \psi_b} \right) H''_{yb} \quad (4.40)$$

3. The Incident Wave

The incident wave has only one component, E'_{yI} , which lies in the y' direction. From Eq. (4.8) its H-vector has the components

$$H'_{xI} = -\frac{k}{\omega\mu_0} \cos \theta_I E'_{yI} \quad (4.41)$$

$$H'_{yI} = 0 \quad (4.42)$$

$$H'_{zI} = \frac{k}{\omega\mu_0} \sin \theta_I E'_{yI} \quad (4.43)$$

4. The Perpendicular Reflected Wave

One of the reflected waves has an E-vector polarized in the y' direction, E'_{y_1} . Equation (4.8) in the primed coordinate system reads as

$$\underline{H}'_1 = \frac{k}{\omega\mu_0} (\sin \theta_I, 0, -\cos \theta_I) \times (0, E'_{y_1}, 0) \quad (4.44)$$

and therefore

$$H'_{x_1} = \frac{k}{\omega\mu_0} E'_{y_1} \cos \theta_I \quad (4.45)$$

$$H'_{y_1} = 0 \quad (4.46)$$

$$H'_{z_1} = \frac{k}{\omega\mu_0} \sin \theta_I E'_{y_1} \quad (4.47)$$

5. The Parallel Reflected Wave

In this case the H-vector has only one component $H'_{y_{II}}$.

Equation (4.9) in the primed coordinate system reads as

$$\underline{E}_{II} = - \frac{k}{\omega\mu_0} (\sin \theta_I, 0, -\cos \theta_I) \times (0, H'_{y_{II}}, 0) \quad (4.48)$$

and the E-field is therefore given by

$$E'_{x_{II}} = - \frac{k}{\omega\mu_0} \cos \theta_I H'_{y_{II}} \quad (4.49)$$

$$E'_{y_{II}} = 0 \quad (4.50)$$

$$E'_{z_{II}} = - \frac{k}{\omega\mu_0} \sin \theta_I H'_{y_{II}} \quad (4.51)$$

Now that the field components parallel to the boundary have been evaluated, they can be substituted into the boundary condition equations to obtain the magnitude of the generated waves as a function of the incident wave amplitude. Continuity of the E'_x , E'_y , H'_x , and H'_y field

components at the boundary give the following four equations:

$$\begin{aligned}
 -\frac{k}{\omega\epsilon_0} \cos\theta_I H'_{y\parallel} &= \frac{m \cos\theta_a}{\sin\psi_a} E''_{ya} + \left(\frac{k_b \cos\psi_b \sin\theta_b}{\omega\epsilon_0 L_1 \sin\psi_b} - \frac{\omega\mu_0}{k_a \sin\psi_b} \right) H''_{yb} \\
 E'_{yI} + E'_{y\perp} &= \frac{n \sin\theta_a - l \cos\theta_a}{\sin\psi_a} E''_{ya} - \frac{m\omega\mu_0}{k_b \sin\psi_b} H''_{yb} \\
 -\frac{k}{\omega\mu_0} (E'_{yI} - E'_{y\perp}) &= -\frac{k_a \cos\theta_a (n \sin\theta_a - l \cos\theta_a)}{\omega\mu_0 \sin\psi_a} E''_{ya} + \frac{m \cos\theta_b}{\sin\psi_b} H''_{yb} \\
 H'_{y\parallel} &= \frac{k_a}{\omega\mu_0} \frac{m}{\sin\psi_a} E''_{ya} + \frac{n \sin\theta_b - l \cos\theta_b}{\sin\psi_b} H''_{yb}
 \end{aligned} \tag{4.52}$$

Solving these equations yields the result

$$E''_{ya} = \frac{d_2}{d_1} E'_{yI} \qquad H''_{yb} = -\frac{d_3}{d_1} E'_{yI} \tag{4.53}$$

where

$$\begin{aligned}
 d_1 &= -\frac{1}{\sin\psi_a \sin\psi_b} \left\{ (n \sin\theta_a - l \cos\theta_a) (N_a \cos\theta_a + \cos\theta_I) \right. \\
 &\quad \left. \left(\frac{N_b \cos\psi_b \sin\theta_b}{L_1} - \frac{l}{N_b} + n \sin\theta_b \cos\theta_I - l \cos\theta_I \cos\theta_b \right) \right. \\
 &\quad \left. + m^2 (\cos\theta_b N_b + \cos\theta_I) (\cos\theta_a + N_a \cos\theta_I) \right\}, \\
 d_2 &= -\frac{2\cos\theta_I}{\sin\psi_b} \left\{ \frac{N_b \cos\psi_b \sin\theta_b}{L_1} - \frac{l}{N_b} + n \sin\theta_b \cos\theta_I - l \cos\theta_I \cos\theta_b \right\},
 \end{aligned} \tag{4.54}$$

$$\tag{4.55}$$

$$d_3 = - \frac{2 \cos \theta_I m}{c \mu_0 \sin \psi_a} (\cos \theta_a + N_a \cos \theta_I) ,$$

$$N_a = k_a c / \omega, \text{ and } N_b = k_b c / \omega . \quad (4.56)$$

E. BOOKER QUARTIC

This section is concerned with the determination of N_a , N_b , θ_a , and θ_b appearing in Eqs. (4.53-4.56). From Eq. (4.23), it follows that

$$N_a = \sqrt{L_1} . \quad (4.57)$$

Snell's law gives us θ_b in the form

$$\sin \theta_a = \frac{\sin \theta_I}{N_a} = \frac{\sin \theta_I}{\sqrt{L_1}} \quad (4.58)$$

The corresponding values for the slow wave follow from a simplified version of the Booker quartic method (Budden, 1966). The dispersion equation for this wave, Eq (4.25), can be rewritten in the form

$$N_b^2 [L_1 + (L_0 - L_1) \cos^2 \psi] = L_0 L_1 \quad (4.59)$$

Substituting the relations

$$N_b \cos \psi = l \sin \theta_I + n (N_b \cos \theta_a) \quad (4.60)$$

$$N_b^2 = \sin^2 \theta_I + (N_b \cos \theta_b)^2 \quad (4.61)$$

into Eq. (4.59) yields the equation

$$L_1 [\sin^2 \theta_I + (N_b \cos \theta_b)^2] + (L_0 - L_1) [l \sin \theta_I + n (N_b \cos \theta_a)]^2 = K_0 K_1 \quad (4.62)$$

which is quadratic in $N_b \cos \theta_b$ and has the solution

$$N_b \cos \theta_b = \frac{(L_1 - L_0) \ln \sin \theta_I + \sqrt{L_1 (L_0 - L_1) [n^2 L_0 - \sin^2 \theta_I (n^2 + l^2) + L_1^2 (L_0 - \sin^2 \theta_I)]}}{L_1 + n^2 (L_0 - L_1)} \quad (4.63)$$

N_b is then determined from Eq. (4.61).

F. DETERMINATION OF FIELD COMPONENTS IN THE UNPRIMED COORDINATE SYSTEM

In order to carry out this computation the components of E_{yb}'' and H_{yb}'' in the original unprimed coordinate system must be determined.

This is done by using Eq. (4.3) to transform the primed components of the previous section into the unprimed system. Starting with Eqs. (4.28-4.30) and (4.35-4.37), the following equations are obtained

$$E_{xa} = \rho_{xa} E_{ya}'' \quad E_{ya} = \rho_{ya} E_{xa}'' \quad E_{za} = \rho_{za} E_{ya}'' \quad (4.64)$$

$$H_{xb} = \rho_{xb} H_{yb}'' \quad H_{yb} = \rho_{yb} H_{xb}'' \quad H_{zb} = \rho_{zb} H_{yb}'' \quad (4.65)$$

where

$$\rho_{xa} = - \frac{k_y \cos \varphi \sin \theta_a}{k_z \sin \psi_a} \quad (4.66)$$

$$\rho_{ya} = \frac{1}{\sin \psi_a} \left[\frac{k_x \cos \varphi \sin \theta_a}{k_z} - \cos \theta_a \sin \varphi \right] \quad (4.67)$$

$$\rho_{za} = \frac{k_y \sin \varphi \sin \theta_a}{k_z \sin \psi_a} \quad (4.68)$$

$$\rho_{xb} = - \frac{k_y \cos \varphi \sin \theta_b}{k_z \sin \psi_a} \quad (4.69)$$

$$\rho_{yb} = \frac{1}{\sin\psi_b} \left[\frac{k_x \cos\varphi \sin\theta_a}{k_\perp} - \cos\theta_a \sin\varphi \right] \quad (4.70)$$

$$\rho_{zb} = \frac{k_y \sin\varphi \sin\theta_b}{k_\perp \sin\psi_b} \quad (4.71)$$

G. FINAL SOLUTION FOR THE FAST ALFVÉN WAVE

First it is necessary to solve for the amplitude of the electric field in the x-direction for the fast wave. Combining Eqs. (4.21), (4.22), (4.53), and (4.64), we obtain

$$E_{xa}(\underline{r}) = - \int_{xa} \frac{d_2}{d_1} \frac{jk_\perp \omega \mu_0 M}{8\pi^2 k_{z0}} \exp\{-j[k_{z0} a + \underline{k} \cdot \underline{r}]\} dk_x dk_y \quad (4.72)$$

where \underline{k} satisfies Eq. (4.23).

If it is assumed that (kr) is very large, it is possible to apply the method of stationary phase along the lines given by Lighthill [1960]. Following Lighthill, it can be shown that an integral of the form

$$E(\underline{r}) = \int F(\underline{k}) \exp(-j\underline{k} \cdot \underline{r}) dk_x dk_y \quad (4.73)$$

when \underline{k} satisfies the dispersion relation

$$D(\underline{k}) = 0 \quad (4.74)$$

can be evaluated in the form

$$E\left(\frac{r \nabla_{\underline{k}} D}{|\nabla_{\underline{k}} D|}\right) = \frac{2\pi}{r\sqrt{K}} F(\underline{k}) \exp(-j\underline{k} \cdot \underline{r}) \quad (4.75)$$

where $\nabla_{\mathbf{k}}$ is the gradient with respect to \mathbf{k} and K is the Gaussian curvature of the surface

$$D(\mathbf{k}) = 0 \quad (4.76)$$

It follows from Eq. (4.23) and the expression given by Lighthill [1960] for K that

$$D = k^2 - \frac{\omega^2 L_1}{c^2}$$

$$\nabla_{\mathbf{k}} D = 2\mathbf{k}$$

$$|\nabla_{\mathbf{k}} D| = 2k$$

$$K = \frac{c^2}{\omega^2 L_1} \quad (4.77)$$

Therefore the final result for $E_{\mathbf{x}\mathbf{a}}$ can be written as

$$E_{\mathbf{x}\mathbf{a}}\left(\frac{\mathbf{k}\mathbf{r}}{k}\right) = - \frac{\rho_{\mathbf{x}\mathbf{a}} d_2}{d_1} \frac{j\omega^2 k_1 \mu_0 M \sqrt{L_1}}{4\pi k_{z0} r c} \exp[-j(k_{z0} \mathbf{a} + \mathbf{k} \cdot \mathbf{r})] \quad (4.78)$$

where

$$k = \frac{\omega}{c} \sqrt{L_1} \quad (4.79)$$

$E_{\mathbf{y}\mathbf{a}}$ and $E_{\mathbf{y}\mathbf{b}}$ are found by merely replacing $\rho_{\mathbf{x}\mathbf{a}}$ by $\rho_{\mathbf{y}\mathbf{a}}$ and $\rho_{\mathbf{z}\mathbf{a}}$, respectively.

H. FINAL SOLUTION FOR THE SLOW ALFVÉN WAVE

Proceeding in the same manner as in the previous section, it may be shown that the H_x field for the slow wave is given by

$$H_{xb}(\underline{r}) = - \int \rho_{xb} \frac{d_3}{d_1} \frac{jk_1 \omega \mu_0 M}{8\pi^2 k_{z0}} \exp \left\{ -j[k_{z0} \underline{a} + \underline{k} \cdot \underline{r}] \right\} d_{kx} d_{ky} \quad (4.80)$$

where \underline{k} satisfies Eq. (4.25). It follows from Eq. (4.25) that D may be written

$$\begin{aligned} D &= (L_0 - L_1) k^2 \cos^2 \psi + L_1 k^2 - \frac{\omega^2}{c^2} L_0 L_1 \\ &= (L_0 - L_1) (\sin \varphi k_x + \cos \varphi k_z)^2 + L_1 k^2 - \frac{\omega^2}{c^2} L_0 L_1 \end{aligned} \quad (4.81)$$

A straightforward calculation then shows that

$$\frac{\nabla_k D}{|\nabla_k D|} = \frac{(L_0 - L_1) \cos \psi_b (\sin \varphi \underline{i}_x + \cos \varphi \underline{i}_z) + L_1 \underline{k}/k}{[(L_0 + L_1)(L_0 - L_1) \cos^2 \psi_b + L_1^2]^{1/2}} \quad (4.82)$$

Following Lighthill [1960], it can also be shown that the Gaussian curvature is given by

$$K = \frac{L_1^3 L_0^2 \omega^2 / c^2}{k^4 [L_0^2 \cos^2 \psi_b + L_1^2 \sin^2 \psi_b]^2} \quad (4.83)$$

It then follows from Eqs. (4.75) and (4.80) that, in the asymptotic limit,

$$H_{xb} \left(\underline{r} \frac{\nabla_k D}{|\nabla_k D|} \right) = - \frac{\rho_{xb} d_3}{d_1} \frac{jk_1 k^2 c \mu_0 M (L_0^2 \cos^2 \psi_b + L_1^2 \sin^2 \psi_b)}{4\pi k_{z0} L_1^{3/2} L_0 r} \exp [-j(\underline{k}_{z0} \underline{a} + \underline{k} \cdot \underline{r})] \quad (4.84)$$

Again, H_{yb} and H_{zb} are found by replacing ρ_{xb} by ρ_{yb} and ρ_{zb} , respectively.

V. SOME PRACTICAL CONSIDERATIONS

The construction of a ground-based current loop large enough to generate hydromagnetic waves in the overhead ionosphere involves certain problems of a practical nature. What kind of wire should be used for the loop, for example? Or, should the wire be raised above the ground on poles? Similarly, the loop requires considerable power while in operation and the handling of this power introduces further problems. Some of these practical details are discussed in this chapter. The object is to show that construction and operation of the current loop is feasible with present technology. A loop with a radius of 10 km and carrying a current of 1000 amps is made the base of our considerations. Larger loops, with greater current-carrying capability, are feasible and will also be discussed. However, it is convenient to have some standard and the smaller loop serves that purpose.

A. DETAILS OF THE LOOP

1. Construction

It is essential that the total resistance of the current loop, and therefore the resistance of the wire comprising it, be kept as low as possible. In other words, the loop should be constructed of thick copper or aluminum wire. There are two major reasons for this requirement. First, the wire must be capable of carrying at least 1000 amp without overheating and, second, the power needed to drive a given current in the loop is directly proportional to the loop resistance and can only be kept small by minimizing the resistance. However, wire resistance is

inversely related to its diameter, whereas its cost is approximately directly related to the diameter. It can be seen, therefore, that there is a trade-off between the wire (and installation) costs and the running (and power conversion) costs for the current loop. We feel that the benefits accruing from an increase in wire size generally outweigh the added cost of the wire. Not only are the running and power conversion costs reduced but, in addition, greater maximum currents are made possible.

The largest available wires are mostly constructed of aluminum or of aluminum over a steel core (the aluminum may be either stranded or unstranded). We would recommend stranded aluminum over a steel core of gauge 2000 mcm (diameter $\approx 1\text{-}3/4$ inches) and with a resistance of approximately $0.03 \Omega/\text{km}$ at 50°C . The total resistance of a 10 km radius loop is then just under 2Ω and the power required to drive 1000 amp is ≈ 2 Megawatts. If the recommended wire is hung off the ground, i.e., in free air, it can carry a maximum current of about 3000 amps. For this large current there would be a rise of about 60°C in the temperature of the wire above the ambient temperature.

Insulated wires are available at increased cost but have the disadvantage in our case that they do not dissipate heat to the surrounding air so readily. Thus, their maximum current-carrying capability is less than that of uninsulated wire of the same gauge. Insulated wire has one advantage in that at a suitable location it could conceivably be laid on the ground. However, this further reduces the ability of the wire to dissipate heat. We consider the most effective loop to be one constructed of uninsulated wire and strung on poles above the ground. The poles add extra expense but are almost unavoidable. For a loop of 10 km radius or larger there will always be roads, streams and other irregularities of

terrain to be crossed, and if the loop was constructed above ice or snow it would have to be supported to prevent it from sinking. The available information suggests that three turns of 2000 mcm gauge wire is probably the maximum number of turns that can be supported on inexpensive wooden poles.

2. Size

In principle there is no limit on the radius of the loop, and there is much to be gained by making the loop as large as possible. Provided the loop can still be treated as a dipole, its moment and magnetic field vary as the square of the radius, whereas the circumference (length of wire) varies with the radius alone. Thus, doubling the radius of the loop increases the field four times (for a given current) but only requires as much extra wire as in the original loop. Once the dimensions start to become comparable to the field point distance, and the loop can no longer be treated as a dipole, increases in the loop radius become less effective. The change is caused by the now non-negligible R^2 term in the denominator of the equation for the axial magnetic field (see equation A.3 in Appendix A). Figure 5.1 shows how the change takes place. Shown in the figure is the variation of the axial magnetic field at 100 km for a loop of constant magnetic moment ($\pi \cdot 10^{11}$ amp. m²) but with a radius varying from 0 km (i.e. dipole) to 150 km. It can be seen that a rapid decrease in magnetic field commences when the radius reaches about 20 km. The rate of decrease is greatest in the radius range 20 - 50 km and becomes less beyond the 50 km point of inflection. However, it should be pointed out that the field produced by the 50 km loop is only about one

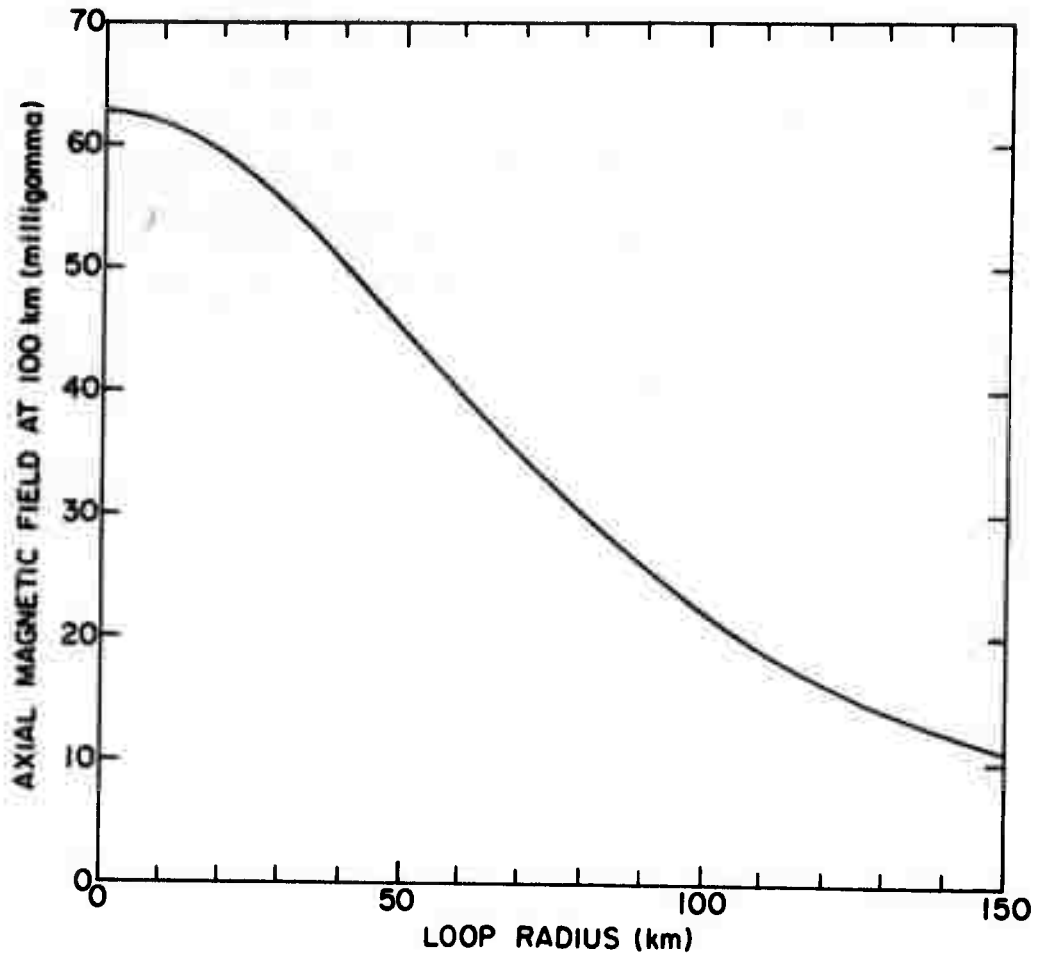


Figure 5.1 Variation of the axial magnetic field at 100 km for a current loop of constant moment ($\pi \cdot 10^{11}$ amp.m²) but variable radius.

third less than the dipole field, whereas the field of the 100 km loop is about half the field of the 50 km loop. In practice, of course, the magnetic moment of the loop increases with increasing radius and greater axial magnetic fields can still be produced by keeping the current unchanged and increasing the radius of the loop. The point is that doubling the loop radius no longer necessarily increases the axial field four times. For example, given a certain fixed loop current, an increase of the loop radius from 50 km to 100 km only doubles the axial magnetic field at 100 km.

With the above considerations in mind, we would limit the radius of the loop to a value in the range 25 - 50 km. The field produced by such a loop can be quite substantial at E-region heights. A three turn loop of radius 50 km carrying a current of 3000 amps has a resistance of about 28Ω (2000 mcm aluminum wire), a loop moment of $225\pi \times 10^{11}$ amp.m² (7.1×10^{13} amp. m²) and, at an altitude of 100 km above the loop, produces an axial field of close to one gamma. This amplitude is large compared with typical magnetic field amplitudes usually associated with micropulsations. The field can be increased still further but with somewhat greater effort and less efficiency. We consider the three-turn loop of 50 km radius, with a maximum current of 3000 amps, to be the limit to what might be comparatively easily achieved. (The power requirement for such a loop is huge, about 250 Mw, but huge powers are available from the utilities and we are here investigating the limits to a practical system).

In the remainder of this chapter the three-turn 50 km radius loop, carrying 3000 amp, will be referred to as "the 50 km loop". The standard single-turn, 10 km radius loop, carrying 1000 amp, will similarly be referred to as "the 10 km loop".

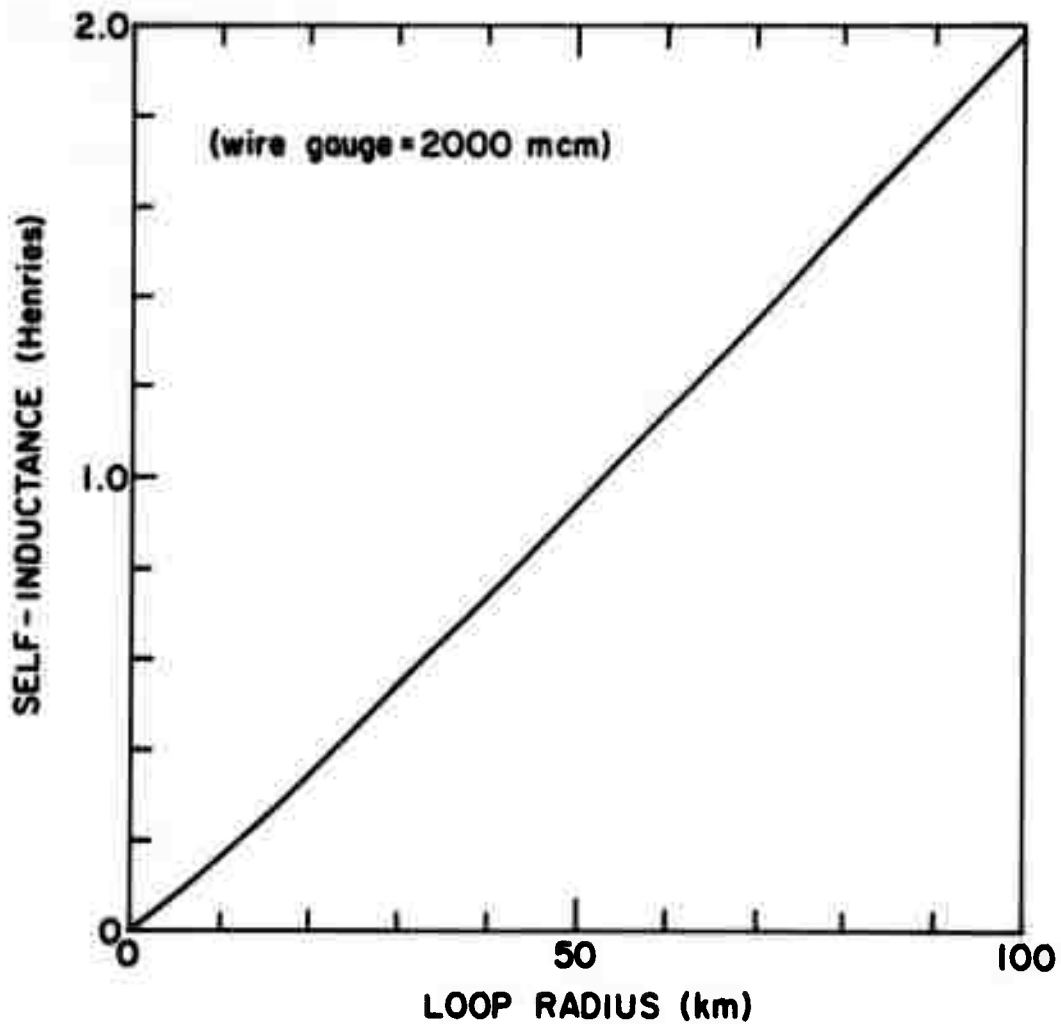


Figure 5.2 Variation of the self-inductance of a single circular loop, constructed of wire of gauge 2000 mcm (diameter \approx 1.75 inches), as the loop radius is increased from about 0 km to 100 km.

3. Self-Inductance

The self-inductance of a single circular loop of radius R and wire radius r is given by

$$L = \mu_0 R \left[\ln\left(\frac{8R}{r}\right) - \frac{7}{4} \right] \quad . \quad (5.1)$$

There are some approximations involved in deriving this formula, but they all appear to be satisfied in this case ($r \ll R$, as required, and the skin effect will be negligible at 1 Hz). Figure 5.2 shows the variation of L for loops varying in radius from ~ 0 km to 100 km and constructed of wire of gauge 2000 mcm. It can be seen that L is roughly proportional to R and varies from 168 mH for a 10 km loop to 1960 mH for a 100 km loop. The inductance values are not exceptionally large. To illustrate, the multi-turn solenoids used to record micropulsations at Stanford are about 5 feet long and 6 inches in diameter and have inductances of ~ 16 H.

The importance of the above self-inductances can be assessed by comparing the ohmic resistance of the coils with their inductive reactances ωL . With 2000 mcm aluminum wire, the resistance of the loop varies from about 2Ω for the 10 km loop to 9.4Ω for a 50 km single-turn loop. The corresponding inductive reactances at 1 Hz vary from about 1Ω to about 6Ω and are always less than the ohmic resistances. These data indicate that the self-inductance of the loops will not interfere significantly with their use as micropulsation generators. On the other hand, the self-inductance effects will not be completely negligible and should be carefully evaluated in any design program.

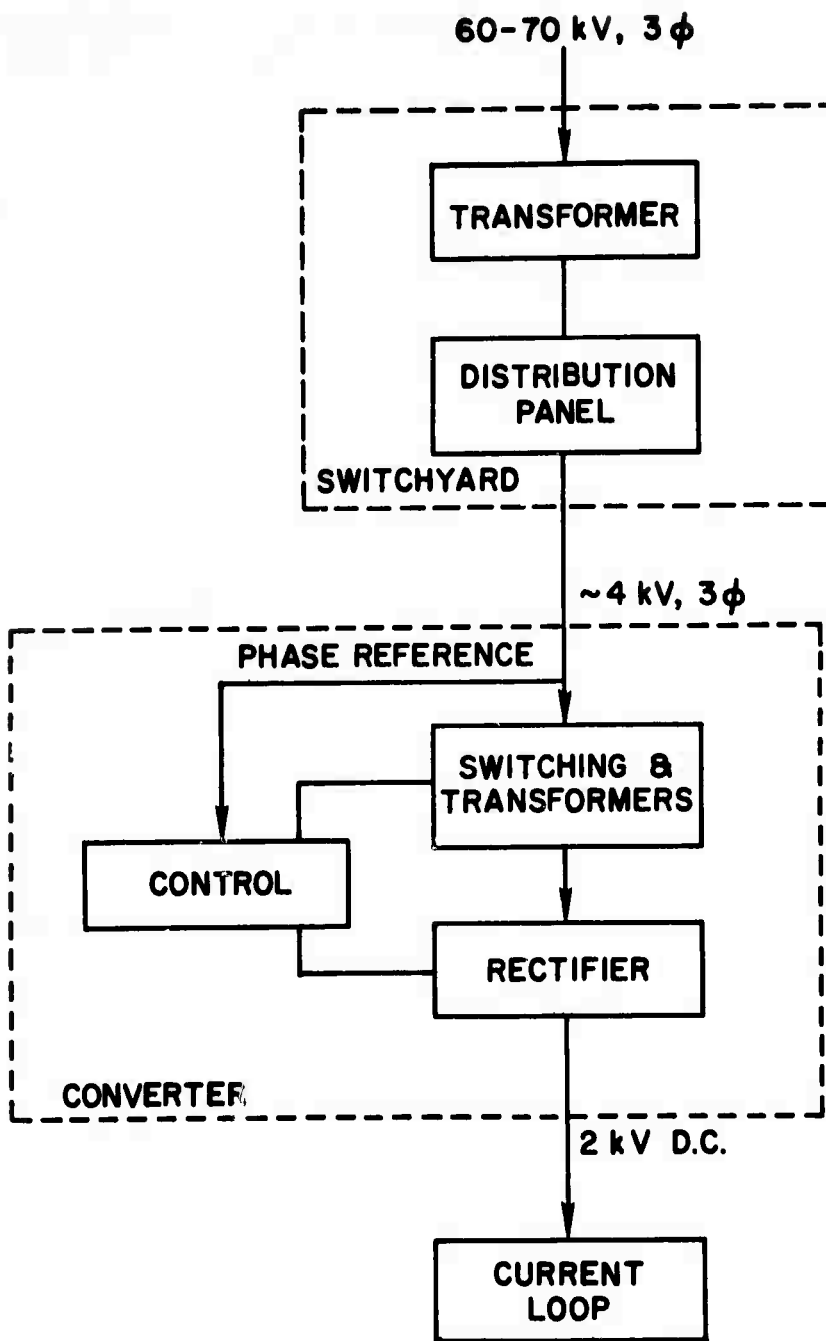


Figure 5.3 Block diagram of a power system for the 10 km loop.

B. POWER MANAGEMENT AND FREQUENCY GENERATION

Early in this study it became clear that there were several alternative ways to produce a large alternating current in a conducting loop. The method we chose to investigate in some detail is probably the most straightforward of these methods: the current is either reversed or switched on and off repetitively by suitable control devices. A "square wave" magnetic field variation is produced with a frequency that is dependent upon the switching rate. We do not assert that this method is necessarily the best for the production of the required large alternating current in the loop. At the same time, the switching method does have a number of desirable features and is worth serious consideration for artificial micropulsation generation.

The major disadvantage of a "square wave" magnetic field variation is the presence of harmonics. These harmonics absorb roughly one quarter (23.4%) of the input power and the higher frequencies (≥ 20 Hz) may also have undesirable interference effects. The overall loss of power is probably the most severe problem. Comparatively little power is absorbed by the higher frequency harmonics, compared to the lower frequency harmonics, and they are more severely attenuated by the earth and ionosphere. Their possible interference effects are thus restricted to an area close to the current loop.

Figure 5.3 shows a block diagram of the power system for the standard 10 km loop. A voltage of close to 2 kV is required to drive the maximum loop current of 1000 amps and it is obtained with little difficulty from the standard 60 - 70 kV power transmission voltage. As shown in the block diagram the voltage entering the system is first

transformed down to a lower value ($\sim 4\text{kV}$) in a switchyard section. The switchyard also serves to protect the power company and the following converter stage. In the converter stage the $\sim 4\text{kV}$ three phase A.C. voltage is converted to the desired switched D.C. voltage that is applied directly to the current loop "antenna". Transformers in the converter section adjust the A.C. voltage to give the required 2kV D.C. voltage amplitude. The control circuitry necessary for all the operations in the converter stage is indicated by a separate block in the diagram.

The resistance of the 50 km loop is about 28Ω and a voltage of close to 80 kV is required to drive the desired maximum current of 3000 amps. It would obviously be very difficult to supply all the voltage and power at one point on the loop. A possible solution is to space several substations around the circumference of the loop with each substation supplying part of the required voltage and having a power system similar to the one shown in Figure 5.3.

C. LOCATION OF THE CURRENT LOOP

The most important positive factor in the choice of a site for the current loop, and we will initially restrict consideration to sites within the continental United States, is either a surface layer of low to medium electrical conductivity or at least only a thin surface layer of high conductivity. Other important factors are (a) suitable location relative to the geomagnetic field; (b) remoteness of the site (to minimize interference with telephone and power circuits); (c) power availability; (d) security (to prevent theft of wire and other components); and (e) low cost.

Naturally-occurring Pc 1 micropulsations usually originate on geomagnetic field lines that extend out to about 4 earth radii or more, at their equatorial points, from the earth's center. For the current loop to be suitably located relative to these field lines it would have to be constructed in Canada or Alaska. While we have no specific objection to either location, it is clear that each has a number of minor disadvantages and no major advantages other than the one discussed. Furthermore, it can be argued that an artificial source of micropulsations does not necessarily have to be located in the most favorable location for the generation of the natural signals. On balance, therefore, we decided that a site south of the Canadian-USA border would be adequate for the current loop.

Factors (b) - (e) all suggest that the site should be in the Western part of the United States where there are large expanses of largely uninhabited desert (often in restricted areas) and where there are large hydroelectric power stations capable of supplying abundant power. However, the surface conductivity of the desert areas is never very low and, in some locations, is undesirably high. Keller et al. (1966) show a surface resistivity map of the United States (Figure 5.4), and the three areas of lowest conductivity are in the New England - Appalachia region, in northern Minnesota, and in a section of the northern Rocky Mountains. In the west and mid-west the conductivity is predominantly quite high. The areas of moderate conductivity in this region occur irregularly between the Sierra Nevada in California (and the Cascade Range to its north) and the eastern termination of the Rocky Mountains. Keller et al. do not indicate the depth of the surface layers whose resistivities are shown in the figure. For the high conductivity areas

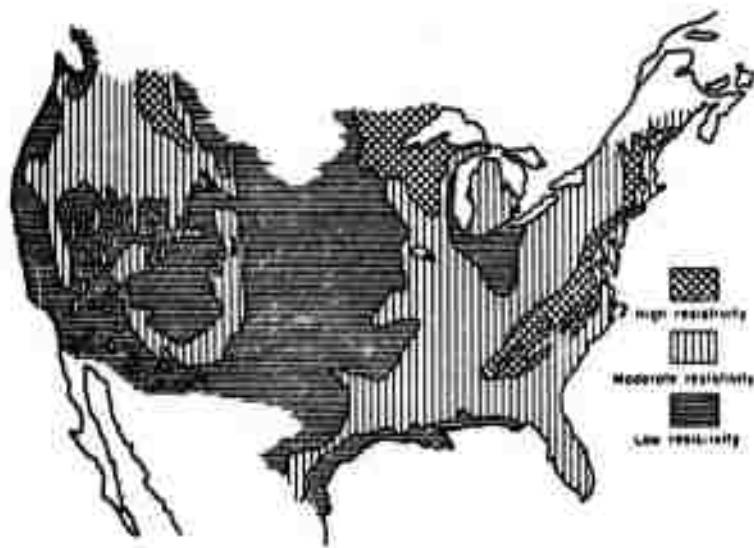


Figure 5.4 Surface resistivity of the United States
(After Keller et al., 1966)

in the west the depth probably varies between 10 m and 1 km [e.g., Jackson (1966)].

The situation in central Nevada is of special interest, because our preliminary investigations indicate that an AEC test site may possibly be available for construction of the current loop. The site in question is restricted to authorized personnel, is presently inactive and has 10 Mw of power capacity already available. The surface layer conductivity in Nevada varies from moderate to high, with the high conductivities mostly confined to the valleys. Jackson's (1966) results indicate that the high conductivity layers are thin relative to their skin depth at micropulsation frequencies. Thus, central Nevada may well be a very suitable location for construction of the current loop.

The only locations outside the United States that may have unique advantages as sites for the current loop are Greenland and Antarctica. Both continents have extremely thick ice sheets resting on rock. From the data in Chapter 3, the ice should have very low conductivity, and if the underlying rock is also of low conductivity (i.e., non-sedimentary rock) either location could be suitable for the current loop. Other advantages are (a) excellent coverage of desirable field lines, (b) practically unlimited level area for construction of the loop, with no right-of-way problems (arrangements would have to be made with the appropriate authorities for the use of either site), (c) few people, and (d) little opportunity for interference with power and telephone circuits. However, while all these advantages are highly desirable, they are not crucial for the success of the current loop experiment. Greenland and Antarctica have one very great disadvantage

at the present time: inadequate power. Until more power can be provided, or the current loop can be made to operate on powers at the kilowatt level (i.e., non-continuous operation), we do not consider Greenland or Antarctica to be feasible sites for the current loop.

D. COST OF A GROUND-BASED CURRENT LOOP SYSTEM

We have obtained preliminary estimates from several companies experienced in heavy electrical engineering for construction of the 10 km loop and its power system. Very briefly, the cost of the loop itself installed on poles varies from \$360,000 to ~\$500,000. Control cabling, lightning cable, and three-phase A.C. lines cost ~\$100,000 and the D.C. converter stage is ~\$200,000. (Two converters are needed, one for the positive and another for the negative voltages, and their cost is ~\$50/Kw). Allowing for labor and contingencies, the cost of the 10 km loop and power system would probably be close to \$1 million.

Projecting the estimates received for the 10 km loop, we estimate a cost of ~\$12 million for the 50 km loop and power system.

These estimates are all preliminary and subject to change. They are included for completeness and to give perspective to the concepts and calculations in this report.

E. ENVIRONMENTAL ASPECTS OF LARGE CURRENT LOOPS

It is probably unnecessary to point out that current loop of the size considered in this report will only be possible in areas that are largely uninhabited. Nevertheless, particular concern must be paid to

to the effect of the magnetic field on both human- and wild-life, on plants, and on telephone and power-line circuits. Fortunately, the magnetic field from a current loop has several features that limit its environmental impact. Perhaps the most important of these features is a very rapid drop-off in the amplitude of the field with distance. In addition, it is advantageous that the field amplitudes are mostly small relative to the geomagnetic field and that their frequency of oscillation is very low.

At distances large compared to the radius of the loop the dipole approximation becomes valid and the field decreases as the inverse cube of distance. Calculations with the finite loop expressions given by Smythe (Appendix A; see Figure 5.5) indicate that in the plane of the loop the dipole approximation is accurate to within about 5 percent at a distance of four times the radius from the center of the loop. (Note that the plane of the loop represents the earth's surface). For the 50 km loop, the field at 200 km (i.e., at $4R$) from the center of the loop is close to 1γ . Magnetic variations of this amplitude and with micropulsation frequencies are not uncommon in the auroral zones and appear to have no harmful effects whatsoever. We will refer to the distance for a 1γ field as the "critical distance".

For distances greater than the critical distance the current loop is likely to have a negligible effect on everything except sensitive magnetometers. Our calculations indicate that the critical distance will vary from approximately 200 km (50 km loop) to about 30 km (10 km loop) for the loop sizes that might be used in micropulsation generation.

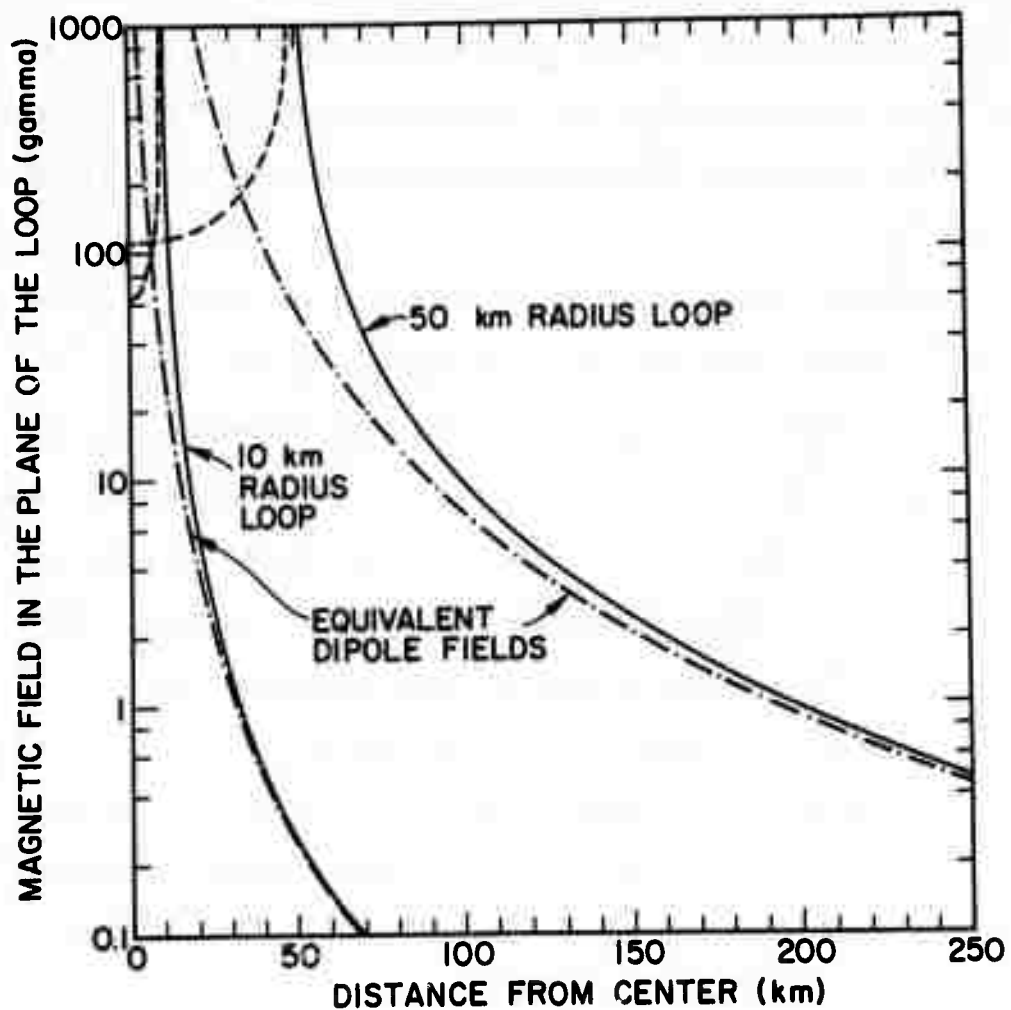


Figure 5.5 Magnetic field variations in the planes of the two current loops discussed in the text. The field inside each of the loops is opposite to the field outside and its variation is indicated by a dashed line. For comparison, the equivalent dipole field variations are also shown.

Figure 5.5 compares the magnetic fields produced in the $z = 0$ plane (i.e., in the plane of each loop) by the 10 km and 50 km loops. The equivalent dipole fields are shown together with the finite loop fields calculated by using equations (A.5) - (A.7) in Appendix A. The magnetic field from a current loop is perpendicular to the plane of the loop at all points, but there is a 180° change of direction if the field at points inside and outside the loop are compared. Figure 5.5 shows that the largest fields produced by the loop occur at the loop surfaces. They do not rise to infinity, as do the dipole fields at the origin, but reach values that may be obtained from Equation (A.8) in Appendix A. Except in the immediate vicinity of the loops themselves (within ~ 12 m for the 50 km loop) the field amplitudes are all less than the earth's magnetic field. It is interesting to compare the fields at the center of the two loops. The field at the center of the 10 km loop is 62.8γ , or about half the 113.1γ field at the center of the 50 km loop. There is a surprisingly small difference in these fields considering that the moment of the 50 km loop is 225 times as large as the moment of the 10 km loop. However, the field at the center of a current loop depends on I/R (see Equation (A.4) in Appendix A) and it can be seen that a simultaneous increase of both the loop current and radius does not necessarily increase the central field, even though the moment of the loop and its field at large distances may be increased substantially.

For distances less than the critical distance it is possible that significant voltages will be generated in telephone or power circuits by the alternating magnetic field of a current loop. A necessary condition, of course, is that the circuits should form closed loops with sufficient

area inside the circle defined by the critical distance. The limited area of strong magnetic field, the low frequencies and the location of the current loop within an uninhabited area will greatly reduce the possibility of interference with telephone and power circuits. Telephone and power lines to facilities close to the current loop, and terminating at those facilities, will very probably be unaffected.

Very little information is available on the effect of weak to moderate alternating magnetic fields (amplitudes $\lesssim 100$ gauss) on plant and animal life. However, there are two good reasons to believe that the magnetic fields produced by the current loop discussed in this report will have no harmful effects. First, the amplitudes of the magnetic field are nearly everywhere very much smaller than the earth's magnetic field. They are many orders of magnitude smaller than some of the magnetic fields commonly encountered in our society, and repeated exposure of human life to these strong fields appears to have negligible effect. Second, the comparatively strong fields existing close to the loop are not unique to these systems. Magnetic fields of similar strength must surround the larger utility lines and yet these fields appear to be quite harmless. In addition, the frequency of variation of these utility fields is considerably higher (~ 60 times) than the frequencies under consideration for the current loop. Assuming that the effect of alternating magnetic fields on plant and animal life is proportional to the induced currents generated by the fields, the effects created by the current loops, if any, must be about sixty times less than those produced by the larger utility lines. Obviously, further consideration should be given to the biological

effects of weak to moderate magnetic fields if a large current loop is ever to be constructed, but at this stage we feel that the magnetic field of such a loop is entirely innocuous.



VI. CONCLUSION

The results presented in the previous chapters indicate that it is technically feasible to construct a current loop on the ground with a magnetic moment as large as 7×10^{13} amp.m² and that such a loop will produce a steady magnetic field of about 1 gamma in the E-region of the ionosphere. Furthermore, this field can be alternated at micropulsation frequencies by switching the loop current. Some of the power input to the loop is dissipated through the generation of harmonics, and earth currents are induced that reduce the magnetic field of the loop. However, at micropulsation frequencies, it still appears possible to produce a magnetic field variation in the E-region with an amplitude of about 1/2 gamma. An artificial 1 Hz field variation of this amplitude is large compared to most natural Pc 1 micropulsation amplitudes observed beneath the ionosphere. It seems reasonable to expect, on this basis, that the alternating magnetic field from the current loop could excite significant Pc 1 hydromagnetic wave amplitudes in the lower ionosphere. Hm waves of other micropulsation frequencies might also be excited by suitable changes in the switching frequency of the current in the loop.

The actual amplitudes of the two hydromagnetic wave modes produced in the E-region by the current loop, i.e., the fast and slow Alfvén waves, can be calculated by using the appropriate expressions derived in Chapter IV. (The magnetic moment M of the loop may be replaced by an "effective" magnetic moment to allow for the generation of harmonics and earth currents). Thus, it is possible to answer the following question: can a current loop

Preceding page blank

with an alternating magnetic moment of amplitude 7×10^{13} amp.m² produce artificial micropulsations at large distances from the loop? To answer this question completely the amplitudes of the two hm modes produced in the E-region must be calculated and their subsequent propagation, and propagation losses, in the ionosphere and magnetosphere considered in some detail. The calculations are lengthy and we restricted ourselves to preliminary estimates of the amplitudes of the hm modes. For the hm mode that is ducted in the ionosphere at Pc 1 frequencies (i.e., the fast Alfvén mode) our estimates indicate that mode amplitudes of at least 1 - 10mγ are achievable with a ground-based current loop of maximum moment 7×10^{13} amp.m². Thus, under nighttime conditions, with little absorption, it should be possible to produce artificial Pc 1 micropulsations with amplitudes greater than 1mγ at large distances from the current loop. This conclusion is independently verified by the work of Greifinger (1972). According to Greifinger, a horizontal magnetic loop with a moment of $\pi \times 10^{13}$ amp.m², located on a single-layered earth of conductivity 1.2×10^{-4} mho/m, can produce an artificial 1 Hz micropulsation of amplitude ~ 7 mγ at a distance of 5000 km from the loop. This result applies only to the hm mode that is ducted in the F-region of the ionosphere and for high-latitude nighttime conditions. However, it confirms that artificial Pc 1 micropulsations can be generated by a ground-based current loop at large distances from the loop.

The theory and calculations included in this report, and in Greifinger's (1972) work, need to be extended in several areas in order to obtain an overall picture of the capability of the current loop. Most pressing,

perhaps, is a complete calculation of the hm energy propagating along a field line to a conjugate point. We are not quite as pessimistic as Greifinger concerning the possibility of completing the required calculation with present knowledge, but it is undoubtedly a complex and difficult problem (c.f. Kitamura and Jacobs, 1968). The calculations also need to be extended to micropulsation frequencies other than Pc 1. For the lowest micropulsation frequencies the single-layered earth model is inadequate and the effect of the earth currents on the performance of the loop should be evaluated by using 2- and 3-layer models.

The loop power system discussed in Chapter V is designed for CW (continuous-wave) operation and there are many advantages to this method of operation. For example, the artificial micropulsations will probably be quite weak at large distances from the loop and a CW signal enables integration to be carried out in a simple and direct manner. Under some circumstances, however, pulsed operation of the loop may have some advantages, particularly when there is a limit on the power available (see Chapter V, Section C). Thus, further engineering studies on the loop power system would be worthwhile.

There have been two other methods proposed for the generation of artificial micropulsations: (a) by using large loop antennas on satellites in the ionosphere and (b) by using large VLF transmitters. The first of these methods avoids the r^{-3} drop-off in magnetic field that occurs between a ground-based current loop and the ionosphere. However, the required loop moment for the generation of hm waves is probably still quite large and it is very difficult to arrange these large moments for satellite-borne loops. The second method, proposed by Bell (1972), is based upon

the precipitation of energetic electrons from the magnetosphere by VLF wave injection. Periodic transmissions from a VLF ground or satellite transmitter are used to precipitate periodic bursts of energetic electrons into the ionosphere. These bursts induce periodic changes in the D- and E-region conductivities, resulting in periodic fluctuations in the currents that flow at these levels and hence micropulsation-like magnetic field changes on the ground. [The precipitating electrons do not appear to generate hm waves in the ionosphere and thus the magnetic field changes do not fit the definition adopted in this report for artificial micropulsations]. There are some disadvantages associated with this method. The periods are likely to be restricted to values greater than about 15 seconds, and the ability of the experimenter to precipitate electrons will depend very greatly upon the variable state of the magnetosphere. Nevertheless, the VLF injection method is interesting.

Another possible method of generating artificial micropulsations is to use an electric dipole instead of the magnetic dipole described in this report. If the moment of the electric dipole is large enough and can be varied at micropulsation frequencies we would expect hm waves to be generated in the overhead ionosphere. We have not calculated the amplitude of the hm modes generated in the ionosphere for an electric dipole; neither have we considered the effect of the earth on the dipole field. However, we consider the electric dipole method for generating micropulsations less likely to be successful than the magnetic dipole method because the technology for producing large currents is much better developed than the technology for large charges. An electric dipole is also more susceptible to the weather than a magnetic dipole. Interestingly, it has been suggested

(Fraser-Smith & Roxburgh, 1969) that the electromagnetic fields produced during lightning discharges may trigger certain Pc 1 micropulsations, and it is well-known that lightning discharges are associated with large electric dipole fields in clouds or between clouds and the earth.

To sum up, it appears possible to generate artificial micropulsations with a large ground-based current loop. The micropulsation frequencies, and to some extent their amplitude, are under the control of the operator of the loop. There are no limits on the time of day, or the state of geomagnetic activity, during which the loop may be used (although the class of micropulsations that the experimenter might wish to generate will vary with time of day and geomagnetic activity). We believe such a loop would significantly advance knowledge of the ULF behavior of the ionosphere and magnetosphere. Also, because there is a limit to what can be achieved by passive observation, the future of micropulsation research is clearly circumscribed without a method of controlled artificial generation. The construction of a current loop generation system, and the possibility of controlled experiments, would greatly expand our knowledge of micropulsation phenomena and provide a powerful new tool for probing both the magnetosphere and the interior of the earth.

APPENDICES

Preceding page blank

Appendix A

MAGNETIC FIELD OF A CURRENT LOOP IN FREE SPACE

1. Dipole Expressions. The magnetic field components for a magnetic dipole of moment \underline{M} directed along the positive z direction of a cylindrical system of coordinates are given by:

$$\begin{aligned} B_r &= \frac{\mu_0 M}{4\pi} \cdot \frac{3rz}{\rho^5} \\ B_\phi &= 0 \\ B_z &= \frac{\mu_0 M}{4\pi} \cdot \frac{2z^2 - r^2}{\rho^5} \end{aligned} \tag{A.1}$$

where $\rho = (z^2 + r^2)^{1/2}$ is the distance from the dipole to the field point.

When the field point is on the z -axis:

$$\begin{aligned} B_r &= 0 = B_\phi \\ B_z &= \frac{\mu_0 M}{2\pi} \cdot \frac{1}{z^3} \end{aligned} \tag{A.2}$$

2. Finite-Loop Expressions. The general expressions for the magnetic field produced by a current loop of finite size are derived by Smythe (1950). They involve elliptic integrals and are quite complicated in their general form. The expressions take a simple form for field points on the axis, however, and it is interesting to compare this simple form with the equivalent dipole expressions.

For a current loop of radius R lying in the $z = 0$ plane of a cylindrical system of coordinates and with its center at the origin we have, for points on the z axis:

$$B_r = 0 = B_\phi$$

$$B_z = \frac{\mu_0 M}{2\pi} \cdot \frac{1}{(z^2 + R^2)^{3/2}} \quad (\text{A.3})$$

where $M = I \cdot \pi R^2$ is the loop moment and it is assumed that the vector moment is directed along the positive z direction. At the center of the loop we have

$$B_{0,0} = \frac{\mu_0 I}{2R} \quad (\text{A.4})$$

When the field points are in the plane of the loop ($z = 0$) the general expressions given by Smythe (1950) for the magnetic field of the loop reduce to

$$B_r = 0 = B_\phi$$

$$B_z = \frac{\mu_0 I}{2\pi} \left[\frac{K}{R+r} + \frac{E}{R-r} \right] \quad (\text{A.5})$$

where K and E are the complete elliptic integrals of the first and second kind, respectively. That is

$$\begin{aligned} K &= \int_0^{\pi/2} [1 - k^2 \sin^2 \theta]^{-1/2} d\theta \\ E &= \int_0^{\pi/2} [1 - k^2 \sin^2 \theta]^{1/2} d\theta \end{aligned} \quad (\text{A.6})$$

with

$$k^2 = \frac{4Rr}{(R+r)^2} \quad (\text{A.7})$$

For $r \approx R$, i.e., for points very close to the wire comprising the loop, equations (A.5) reduce to

$$B_r = 0 = B_\phi$$

$$B_z = \frac{\mu_0 I}{2\pi(R-r)} \quad (\text{A.8})$$

where the equation for B_z is now identical to the equation for the field produced at distance $\Delta r = (R-r)$ by a straight wire carrying a current I .

3. Comparison of the Dipole and Finite-Loop Fields. For large values of z , i.e., large compared to the loop radius R , the axial field of the finite loop will obviously approximate the axial field for a dipole. Even when z is only a little larger than the loop radius it is often still a good approximation to use the dipole expression for the axial field. Consider a particular example that is relevant to the subject of this report. Suppose the moment of both the loop and the dipole is $\pi \cdot 10^{11}$ amp.m², with the loop having a radius of 10 km and carrying a current of 1000 amp. At $z = 100$ km ($z = 10R$) the dipole field is 62.8×10^{12} wb/m², or 62.8 mγ. The equivalent field for the loop is 61.9 mγ. Thus, there is little difference between the two field magnitudes at a distance equivalent to the height of the ionospheric E-region.

The difference between the two fields for a loop of radius 100 km may also be of interest. The loop in this case can only have a current of 10 amp if the moment is to be the same as before. For this example the loop field at 100 km ($z = R$) is 22.2 mγ, or about one third the dipole field.

APPENDIX B

ALTERNATIVE EXPRESSIONS FOR THE TOTAL MAGNETIC
FIELD PRODUCED BY A GROUND-BASED CURRENT LOOP

It follows from equations (3.38) and (3.45) that the total magnetic field for $z > 0$ has components

$$\begin{aligned} B_r &= \frac{\mu_0 M_0}{4\pi} \int_0^\infty F(\omega, \sigma, \lambda) e^{-\lambda z} J_1(\lambda r) \lambda^2 d\lambda \\ B_z &= \frac{\mu_0 M_0}{4\pi} \int_0^\infty F(\omega, \sigma, \lambda) e^{-\lambda z} J_0(\lambda r) \lambda^2 d\lambda \end{aligned} \quad (B.1)$$

where

$$F(\omega, \sigma, \lambda) = 1 - \frac{a^2 + b^2 - \lambda^2}{(a + \lambda)^2 + b^2} \quad (B.2)$$

and a and b are defined by equations (3.44). The right hand side of equation (B.2) can be simplified considerably by using $b^2 = a^2 - \lambda^2$, for then

$$1 - \frac{a^2 + b^2 - \lambda^2}{(a + \lambda)^2 + b^2} = \frac{2\lambda(a + \lambda)}{(a + \lambda)^2 + b^2} = \frac{2\lambda}{(a + \lambda) + (a - \lambda)} = \frac{\lambda}{a} .$$

Thus,

$$F(\omega, \sigma, \lambda) = \frac{\lambda}{a} . \quad (B.3)$$

Consider the equation for a in more detail. This equation may be written

$$a^2 = \frac{\lambda^2}{2} \left[1 + \left(1 + \frac{2}{\delta^4 \lambda^4} \right)^{1/2} \right]$$

where equation (3.0) for the skin depth δ has been used.

If $\frac{2}{\delta^2 \lambda^2} \gg 1$ the equation for a reduces to

$$\begin{aligned} a^2 &\approx \frac{\lambda^2}{2} \left[1 + \frac{2}{\delta^2 \lambda^2} \right] \\ &\approx \frac{\lambda^2}{2} \cdot \frac{2}{\delta^2 \lambda^2} \\ &\approx \delta^{-2} \end{aligned}$$

Thus

$$F(\omega, \sigma, \lambda) \approx \lambda \delta \quad . \quad (B.4)$$

The components of total magnetic field become

$$\begin{aligned} B_r &= \frac{\mu_0 M_0 \delta}{4\pi} \int_0^\infty e^{-\lambda z} J_1(\lambda r) \lambda^3 d\lambda \\ B_z &= \frac{\mu_0 M_0 \delta}{4\pi} \int_0^\infty e^{-\lambda z} J_0(\lambda r) \lambda^3 d\lambda \quad . \quad (B.5) \end{aligned}$$

On the axis of the loop, equations (B.5) give

$$\begin{aligned} B_r &= 0 \\ B_z &= \frac{\mu_0 M_0 \delta}{4\pi} \cdot \frac{6}{z^4} \quad (B.6) \end{aligned}$$

where

$$\int_0^{\infty} e^{-\lambda z} \lambda^3 d\lambda = \frac{3!}{z^4} .$$

Equations (B.6) show that B_z on the axis varies with frequency and conductivity as $(\omega\sigma)^{-1/2}$, provided the approximation $\frac{2}{\delta^2 \lambda^2} \gg 1$ is valid. For $z = 100$ km and $M_0 = \pi \cdot 10^{11}$ amp.m² we obtain

$$B_z = \frac{2.37}{(\omega\sigma)^{1/2}} \text{ m}\gamma . \quad (\text{B.7})$$

Equations (B.5) and (B.6) are convenient alternative expressions for the total magnetic field produced by the ground-based loop (with the earth assumed to be a single layer of conductivity σ).

We now investigate the conditions for equations (B.5) and (B.6) to be valid. The condition $\frac{2}{\delta^2 \lambda^2} \gg 1$ may be written $\lambda \ll \delta^{-1}$. Suppose λ_1 is a value of λ that can be considered much smaller than δ^{-1} , i.e., $\lambda_1 = \epsilon \delta^{-1}$, where ϵ is less than 1. Each of the integrals in equations (B.1) can then be written in the form

$$\int_0^{\lambda_1} [I] d\lambda + \int_{\lambda_1}^{\infty} [I] d\lambda$$

where I is the integrand. The approximation (B.4) is valid in the first integral, but not in the second. However, provided $\lambda_1 z \gg 1$, the second integral will be very small because of the $e^{-\lambda z}$ factor in

the integrand and may be neglected. Thus, the condition for (B.5) and (B.6) to be valid is

$$z \gg \frac{1}{\lambda_1}$$

or

$$z \gg \text{skin depth}$$

Appendix C

FOURIER TRANSFORM OF LOOP CURRENT

Referring to the coordinate system in Figure C.1, the J_x component of the loop current is given by the expression

$$J_x = -I\delta(z+a) \delta(r-R) \sin \phi \quad (C.1)$$

and therefore its Fourier transform is given by

$$J_{xk} = -\frac{I}{8\pi^3} \int r dr d\phi dz \delta(z+a) \delta(r-R) \sin \phi \exp j [k_{\perp} r \cos(\phi-\lambda) + k_z z] \quad (C.2)$$

where (r, ϕ, z) and $(k_{\perp}, \lambda, k_z)$ are polar coordinates for \underline{r} and \underline{k} and δ is the Dirac delta function. Write $\sin \phi$ as

$$\sin \phi = \sin(\phi - \lambda) \cos \lambda + \cos(\phi - \lambda) \sin \lambda \quad (C.3)$$

and note from symmetry that the first term will give no contribution to the integral. Integrating the resulting equation yields

$$J_{xk} = -\frac{2\pi j R^2 I k_y}{8\pi^3 k_{\perp} R} - J_1(k_{\perp} R_0) \exp(-jk_z a) \quad (C.4)$$

In similar fashion

$$J_{yk} = \frac{2\pi j R^2 I k_x}{8\pi^3 k_{\perp} R} - J_1(k_{\perp} R_0) \exp(-jk_z a) \quad (C.5)$$

Equations (C.4) and (C.5) lead immediately to the result

$$\underline{J}_k = -\frac{2jk_x M}{8\pi^3 k_{\perp} R} J_1(k_{\perp} R_0) \exp(-jk_z a) \quad (C.6)$$

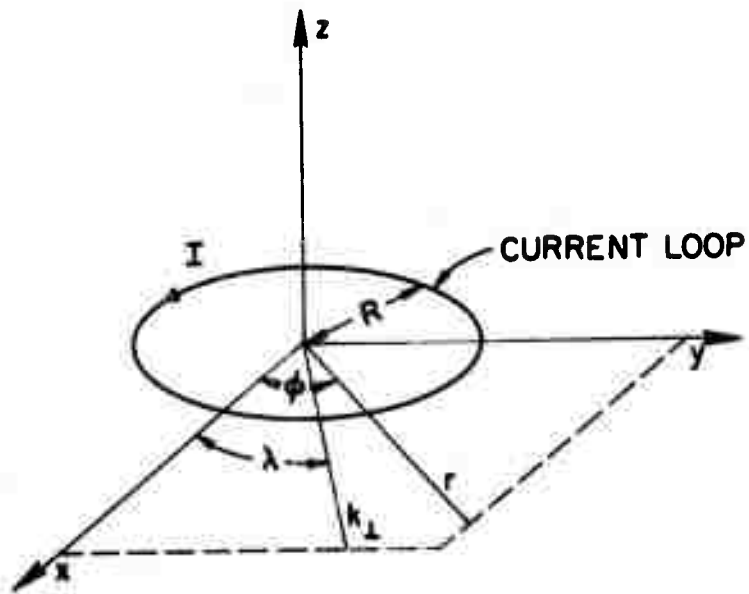


Figure C.1 Coordinate system for calculating the Fourier transform of the loop current.

where

$$\underline{M} = \pi R^2 I \underline{i}_z \quad (C.7)$$

and \underline{i}_z is the unit vector in the z-direction. Only the case where $k_{\perp} R \ll 1$ is of interest, and therefore

$$\underline{J}_{\perp k} = - \frac{j k \times \underline{M}}{8\pi^3} \exp(-j k_z a) \quad (C.8)$$

is obtained as the final result.

REFERENCES

- Bell, T. F., "The production of micropulsations using VLF transmitters", paper presented at the URSI Spring meeting, Washington D.C., April 1972.
- Bhattacharyya, B. K., "Electromagnetic induction in a two-layer earth", J. Geophys. Res., 60, 279, 1955.
- Bomke, H. A., I. A. Balton, H. H. Grote, and A. K. Harris, "Near and distant observations of the 1962 Johnston Island high-altitude nuclear tests", J. Geophys. Res., 69, 3125, 1964.
- Bowman, G. G. and J. S. Mainstone, "Geomagnetic and ionospheric effects at Brisbane following the nuclear explosion on July 9, 1962", Australian J. Phys., 17, 409, 1964.
- Budden, K. G., Radio Waves in the Ionosphere, 542 pp., Cambridge Univ. Press, London, 1966.
- Campbell, W. H., "Geomagnetic Pulsations", in Physics of Geomagnetic Phenomena, edited by S. Matsushita and Wallace H. Campbell, 1398 pp., Academic Press, New York, 1967.
- Campbell, W. H. and T. C. Thornberry, "Propagation of Pc 1 hydromagnetic waves across North America", J. Geophys. Res., 77, 1941, 1972.
- Cantwell, T., and T. R. Madden, "Preliminary report on crustal magnetotelluric measurements", J. Geophys. Res., 65, 4202, 1960.
- Carlson, H. C., W. E. Gordon and R. L. Showen, "High frequency induced enhancements of the incoherent scatter spectrum at Arecibo", J. Geophys. Res., 77, 1242, 1972.

Preceding page blank

- Carpenter, D. L., A. C. Fraser-Smith, R. S. Unwin, E. W. Hones, Jr.,
and R. R. Heacock, "Correlation between convection electric fields
in the nightside magnetosphere and several wave and particle
phenomena during two isolated substorms", J. Geophys. Res., 76,
7778, 1971.
- Clemmow, P. C., and J. C. Dougherty, Electrodynamics of Particles and
Plasmas, 457 pp., Addison-Wesley, Massachusetts, 1969.
- Cornwall, J. M., "Cyclotron instabilities and electromagnetic emission
in the ultra low frequency and very low frequency ranges",
J. Geophys. Res., 70, 61, 1965.
- Crook, G. M., E. W. Greenstadt and G. T. Inouye, "Distant electromagnetic
observations of the high-altitude nuclear detonation of July 9, 1962",
J. Geophys. Res., 68, 1781, 1963.
- Evans, S., "Dielectric properties of ice and snow - a review",
J. Glaciology, 5, 773, 1965.
- Francis, W. E., and R. Karplus, "Hydromagnetic waves in the ionosphere",
J. Geophys. Res., 65, 3593, 1960.
- Fraser-Smith, A. C., "Narrow frequency bands in hydromagnetic emissions
(Pc 1)", J. Atmos. Terr. Phys., 29, 1541, 1967.
- Fraser-Smith, A. C. and K. R. Roxburgh, "Triggering of hydromagnetic
'whistlers' by sferics", Planet. Space Sci., 17, 1310, 1969.
- Gordon, A. N., "The field induced by an oscillating magnetic dipole
outside a semi-infinite conductor", Quart. J. Mech. and Applied Math.,
4, 106, 1951.

- Green, A. W., Jr., B. H. List and J. F. P. Zengel, "The theory, measurement, and applications of very-low-frequency magnetotelluric variations", Proc. I. R. E., 50, 2347, 1962.
- Greifinger, C., and P. S. Greifinger, "Theory of hydromagnetic propagation in the ionospheric waveguide", J. Geophys. Res., 73, 7473, 1968.
- Greifinger, C., "On the feasibility of artificial generation of micropulsations", Sci. Rept. RDA-TR-044-ARPA, Contract DAAH01-71-C-1156, Advanced Res. Proj. Agency, February 1972.
- Helliwell, R. A., J. P. Katsufakis, and M. L. Trimpi, "Whistler-induced amplitude anomalies in VLF propagation", paper presented at the Long Radio Wave Propagation Symposium, U. S. Naval Research Lab., Washington, D.C., April 1972.
- Jackson, D. B., "Deep resistivity probes in the southwestern United States", Geophys., 31, 1123, 1966.
- Jacobs, J. A., and T. Watanabe, "Propagation of hydromagnetic waves in the lower exosphere and the origin of short period geomagnetic pulsations", J. Atmos. Terr. Phys., 24, 413, 1962.
- Jacobs, J. A., Y. Kato, S. Matsushita and V. A. Troitskaya, "Classification of geomagnetic micropulsations", J. Geophys. Res., 69, 180, 1964.
- Jacobs, J. A., "Geomagnetic Micropulsations" in Physics and Chemistry in Space, Vol. 1, 179 pp., Springer-Verlag, New York, 1970.
- Keller, G. V., L. A. Anderson and J. I. Prichard, "Geological survey investigations of the electrical properties of the crust and upper mantle", Geophys., 31, 1078, 1966

- Kitamura, T., and J. A. Jacobs, "Ray paths of Pc 1 waves in the magnetosphere", Planet. Space Sci, 16, 863, 1968.
- Kovach, R. L., and A. Ben-Menahem, "Analysis of geomagnetic micropulsations due to high-altitude nuclear explosions", J. Geophys. Res., 71, 1427, 1966.
- Liemohn, H. B., "Cyclotron-resonance amplification of VLF and ULF whistlers", J. Geophys. Res., 72, 39, 1967.
- Lighthill, M. J., "Studies on magneto-hydrodynamic waves and other anisotropic wave motions", Phil. Trans. Roy. Soc., 252, 397, 1960.
- Mann, J. E., Jr., "A theoretical magnetotelluric problem exhibiting effects of lateral conductivity variations and finite field dimensions", J. Geophys. Res., 72, 2885, 1967.
- Mott, H., and A. W. Biggs, "Very-low-frequency propagation below the bottom of the sea", IEEE Trans., Antennas & Propagation, AP-11 323, 1963.
- Panofsky, W. K. H., and M. Phillips, Classical Electricity and Magnetism, 494 pp., Addison-Wesley, Massachusetts, 1962.
- Price, A. T., "Electromagnetic induction in a semi-infinite conductor with a plane boundary", Quart. J. Mech. and Applied Math., 3, 385, 1950.
- Price, A. T., "The theory of magnetotelluric methods when the source field is considered", J. Geophys. Res., 67, 1907, 1962.
- Ryu, J., H. F. Morrison, and S. H. Ward, "Electromagnetic fields about a loop source of current", Geophys., 35, 862, 1970.

- Smythe, W. R., Static and Dynamic Electricity, 616 pp., McGraw-Hill, New York, 1950.
- Sneddon, I. N., Special Functions of Mathematical Physics and Chemistry, 164 pp., Oliver & Boyd, London, 1956.
- Troitskaya, V. A., "Pulsations of the earth's electromagnetic field with periods of 1 to 15 seconds and their connection with phenomena in the high atmosphere", J. Geophys. Res., 66, 5, 1961.
- Troitskaya, V. A., "Micropulsations and the state of the magnetosphere", in Solar-Terrestrial Physics, edited by J. W. King and W. S. Newman. 390 pp., Academic, New York, 1967.
- Utlaut, W. F., "An ionospheric modification experiment using very high power, high frequency transmission", J. Geophys. Res., 75, 6402, 1970.
- Wait, J. R., "Theory of magneto-telluric fields", J Res. NBS, 66D, 509, 1962.
- Weaver, J. T., "Electromagnetic induction in a two-layer earth", Pacific Naval Laboratory Report 64-1, Defense Research Board, Canada, May 1964.